iScience

CellPress

Article

The Circadian Clock Protein CRY1 Is a Negative Regulator of HIF-1α

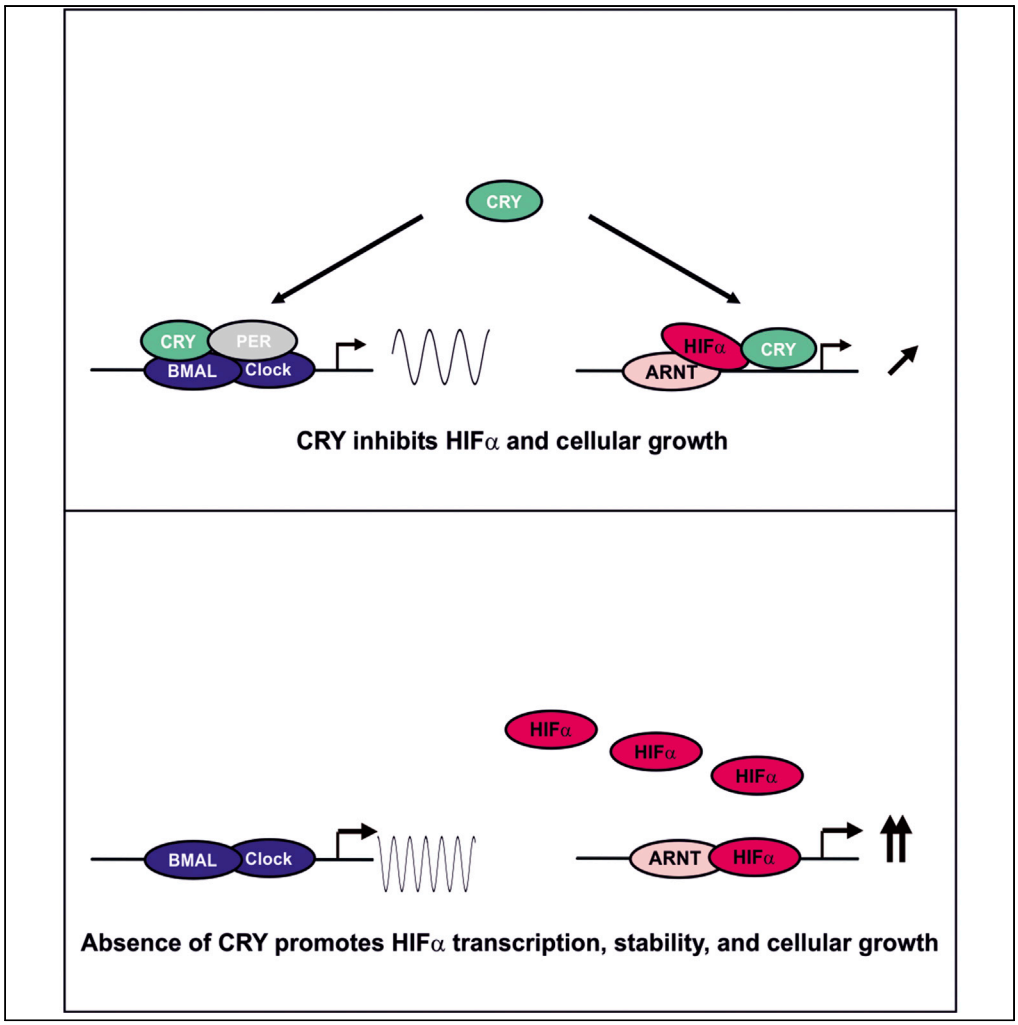

Elitsa Y. Dimova, Mirza Jakupovic, Kateryna Kubaichuk, ..., Ines Chaves, Gijsbertus van der Horst, Thomas Kietzmann

elitsa.dimova@oulu.fi (E.Y.D.)
thomas.kietzmann@oulu.fi (T.K.)

HIGHLIGHTS

Hypoxia and HIFs affect the circadian rhythm

CRY1 directly interacts with both HIF-1α and HIF-2α

CRY1 inhibits binding of HIFs to its target gene promoters

The CRY1-HIFα interaction has opposite roles on cellular growth and migration

Dimova et al., iScience *13*, 284–304
March 29, 2019 © 2019 The Author(s).
https://doi.org/10.1016/j.isci.2019.02.027

iScience

CellPress

Article

The Circadian Clock Protein CRY1 Is a Negative Regulator of HIF-1α

Elitsa Y. Dimova,[1,6,*] Mirza Jakupovic,[2,6] Kateryna Kubaichuk,[1] Daniela Mennerich,[1] Tabughang Franklin Chi,[1] Filippo Tamanini,[3] Małgorzata Oklejewicz,[3] Jens Hänig,[4] Nadiya Byts,[1] Kari A. Mäkelä,[5] Karl-Heinz Herzig,[5] Peppi Koivunen,[1] Ines Chaves,[3] Gijsbertus van der Horst,[3] and Thomas Kietzmann[1,7,*]

SUMMARY

The circadian clock and the hypoxia-signaling pathway are regulated by an integrated interplay of positive and negative feedback limbs that incorporate energy homeostasis and carcinogenesis. We show that the negative circadian regulator CRY1 is also a negative regulator of hypoxia-inducible factor (HIF). Mechanistically, CRY1 interacts with the basic-helix-loop-helix domain of HIF-1α via its tail region. Subsequently, CRY1 reduces HIF-1α half-life and binding of HIFs to target gene promoters. This appeared to be CRY1 specific because genetic disruption of CRY1, but not CRY2, affected the hypoxia response. Furthermore, CRY1 deficiency could induce cellular HIF levels, proliferation, and migration, which could be reversed by CRISPR/Cas9- or short hairpin RNA-mediated HIF knockout. Altogether, our study provides a mechanistic explanation for genetic association studies linking a disruption of the circadian clock with hypoxia-associated processes such as carcinogenesis.

INTRODUCTION

A number of epidemiological studies showed that disturbances of the circadian rhythm strongly correlate with carcinogenesis and tumor progression in humans (for review see Fu and Lee, 2003; Filipski and Levi, 2009; Sahar and Sassone-Corsi, 2009; Rana and Mahmood, 2010). Accordingly, the International Agency for Research on Cancer classified shift work as a group 2A carcinogenic factor (Straif et al., 2007).

The circadian rhythm in mammals is maintained by an integrated network of the central (neural or brain) and peripheral (tissue-specific) clocks. The central clock is located in the suprachiasmatic nucleus of the brain, receives light cues to keep in phase with the light-dark cycle, and synchronizes the peripheral clocks in various tissues through a variety of electrical, endocrine, and metabolic signaling pathways (Albrecht, 2012; Richards and Gumz, 2012). At the genetic level, both the central and the peripheral clocks are regulated by an interplay of positive and negative feedback loops involving the same set of clock genes (Yagita et al., 2001). Thereby, the bHLH-PAS transcription factors CLOCK (circadian locomotor output cycles kaput) and BMAL1 (brain-muscle Arnt-like protein 1) represent the major components of the core clock's positive limb. They induce, among others, the expression of the proteins PER (period 1,2) and CRY (cryptochrome 1,2), which constitute the major arm of the negative limb. The induced PER and CRY proteins then form a complex with each other as well as with modulator proteins such as CK1ε, CKII, or FBXL3 and act as repressors of CLOCK/BMAL heterodimers. Subsequently, they inhibit their own expression as well as those of other CLOCK/BMAL-regulated output genes (Griffin et al., 1999; Kume et al., 1999; Yoo et al., 2005; Sato et al., 2006). The core loop is interconnected to several other feedback loops, including those of REV-ERBs or PPARα/RORs, which repress or activate BMAL1 expression, respectively (Albrecht, 2012; Ko and Takahashi, 2006; Asher and Schibler, 2011). Overall, the continuous interplay between the core CLOCK/BMAL1 positive limb and the PER/CRY negative limb in concert with post-translational modifications and interconnected loops results in the oscillation of gene expression in a circadian manner.

Several recent studies have linked clock function with the cell cycle and reported that clock components, such as PER1, PER2, BMAL1, and CRY1/2 decrease cell proliferation or improve the action of anti-cancer drugs in different cancer cell lines. Moreover, certain types of human cancer show an altered expression of circadian clock genes (reviewed in Shostak, 2017).

In addition to disturbances of the circadian clock, most, if not all, solid tumors display hypoxic areas. Hypoxia has been shown to be the major driver of tumor angiogenesis and a critical determinant for

[1]Faculty of Biochemistry and Molecular Medicine and Biocenter Oulu, University of Oulu, P.O. Box 3000, 90014 Oulu, Finland

[2]Department of Biochemistry, University of Kaiserslautern, 67663 Kaiserslautern, Germany

[3]Department of Molecular Genetics, Erasmus University Medical Center, Wytemaweg 80, 3015CN Rotterdam, the Netherlands

[4]Novartis Pharma GmbH, 97082 Würzburg, Germany

[5]Biocenter Oulu, Department of Physiology, University of Oulu, 90014 Oulu, Finland

[6]These authors contributed equally

[7]Lead Contact

*Correspondence: elitsa.dimova@oulu.fi (E.Y.D.), thomas.kietzmann@oulu.fi (T.K.)

https://doi.org/10.1016/j.isci.2019.02.027

 © 2019 The Author(s).
This is an open access article under the CC BY-NC-ND license (http://creativecommons.org/licenses/by-nc-nd/4.0/).

proliferation, cell growth, and apoptosis (Semenza, 2017; Masson and Ratcliffe, 2014; Kaelin and Ratcliffe, 2008). Mechanistically, a group of the bHLH-PAS family transcription factors called hypoxia-inducible transcription factors, among which hypoxia-inducible factor (HIF)-1α is the best characterized, mediate the transcriptional adaptation to hypoxia. Thereby, HIF-1α together with its binding partner HIF-1β (also known as aryl hydrocarbon receptor nuclear translocator, ARNT) binds to hypoxia-response elements (HREs) within the promoters of numerous hypoxia-responsive genes (Semenza, 2017, Masson and Ratcliffe, 2014; Kaelin and Ratcliffe, 2008).

The disruption of the circadian rhythm in patients with cancer and the appearance of hypoxia in tumors raises the question whether and how the deregulation of the circadian clock system has an impact on the hypoxia response. Several findings suggested a cross talk between the circadian clock and the hypoxia signaling pathway (Hogenesch et al., 1998; Chilov et al., 2001; Eckle et al., 2012), but the mechanisms behind are not completely understood and have just started to emerge. Recent reports have shown that the modulation of oxygen levels can reset the circadian clock at the positive limb in a HIF-1α-dependent manner (Adamovich et al., 2017) and that HIF-1α and BMAL1 engage in a synergistic cross talk (Wu et al., 2017), which adapts anaerobic metabolism in skeletal muscle (Peek et al., 2017). Although these findings favor the view that this cross talk is bidirectional and would eventually also involve the negative arm of the circadian key players, their participation, in particular that of CRY proteins, remains unknown. In the current study we broaden this view by showing that CRY1, but not CRY2, acts as a repressor of HIFs. This occurs via a specific protein-protein interaction that reduces the binding of HIFs at the HREs of target gene promoters and by altering HIF half-life. Disruption of the CRY1-HIF cross talk at the cellular level shows that CRY1 and HIF-1α have an opposite action on cell growth.

Overall, our study identifies a new level of control that links defects in the circadian clock system with hypoxia signaling and carcinogenesis.

RESULTS

Hypoxia Affects the Circadian Rhythm *In Vivo*

To study the possible interplay between the circadian clock and hypoxia we measured the circadian behavior of mice under normoxia (21% O_2) and hypoxia (17% O_2) at 12 h + 12 h light/dark (LD) cycles and at constant darkness (dark/dark; DD). When mice were kept under both normoxia and hypoxia at LD they showed circadian periodicity (Figures 1A and 1B). Intriguingly, we observed that mice at DD lost their circadian rhythm (Figures 1A and 1B) and expressed HIF target genes when exposed to hypoxia (Figure 1C). Together, these data indicate that hypoxia is able to modulate the circadian rhythm.

The Cell-Autonomous Circadian Oscillation in NIH3T3 Cells Is Affected by HIF-1α or HIF-2α

As the hypoxia-mediated loss of the circadian rhythm in mice at DD stems from systemic and cell-autonomous oscillator effects, we next tested to what extent hypoxia affects the cell-autonomous clock. To do this, we first verified the effect of chronic hypoxia (3% O_2 for 32 h) in synchronized Per2:Luc-transfected fibroblasts, which possess a cell-autonomous and self-sustained circadian clock (Yagita et al., 2001; Balsalobre et al., 1998). We found that hypoxia affected the circadian rhythm in two ways, first by reducing the amplitude and second by shortening the period by about 30 min (Figures 2A and 2B). Given that the response to hypoxia is mainly mediated by an increased abundance of the transcription factors HIF-1α and HIF-2α, we next investigated how HIF-1α or HIF-2α affect the circadian clock. To do this, we first cotransfected an expression vector for a hypoxia-mimicking hydroxylation-resistant HIF-1α variant (P/P/N) (Flügel et al., 2012) with the circadian rhythm reporter Bmal1:Luc and analyzed circadian rhythmicity. Similar to hypoxia, overexpression of HIF-1α shortened the circadian period and reduced the amplitude (Figures 2C and 2D). Overexpression of HIF-2α showed a similar response (Figures S1A and S1B). In contrast to hypoxia and HIFs, the non-specific prolyl hydroxylase inhibitor dimethyloxalylglycine (DMOG), which is often considered as a hypoxia mimetic, lengthened the period (Figures S1C and S1D). Together, these data indicate that HIF-1α and HIF-2α mimic the effect of hypoxia on the circadian clock, whereas the DMOG effects appear to be HIF independent.

The Circadian Oscillation of PAI-1 Is Affected by Hypoxia

The aforementioned observations appear to be important for genes that are responsive to both hypoxia and the circadian clock. The *SERPINE1* gene encoding plasminogen activator inhibitor-1

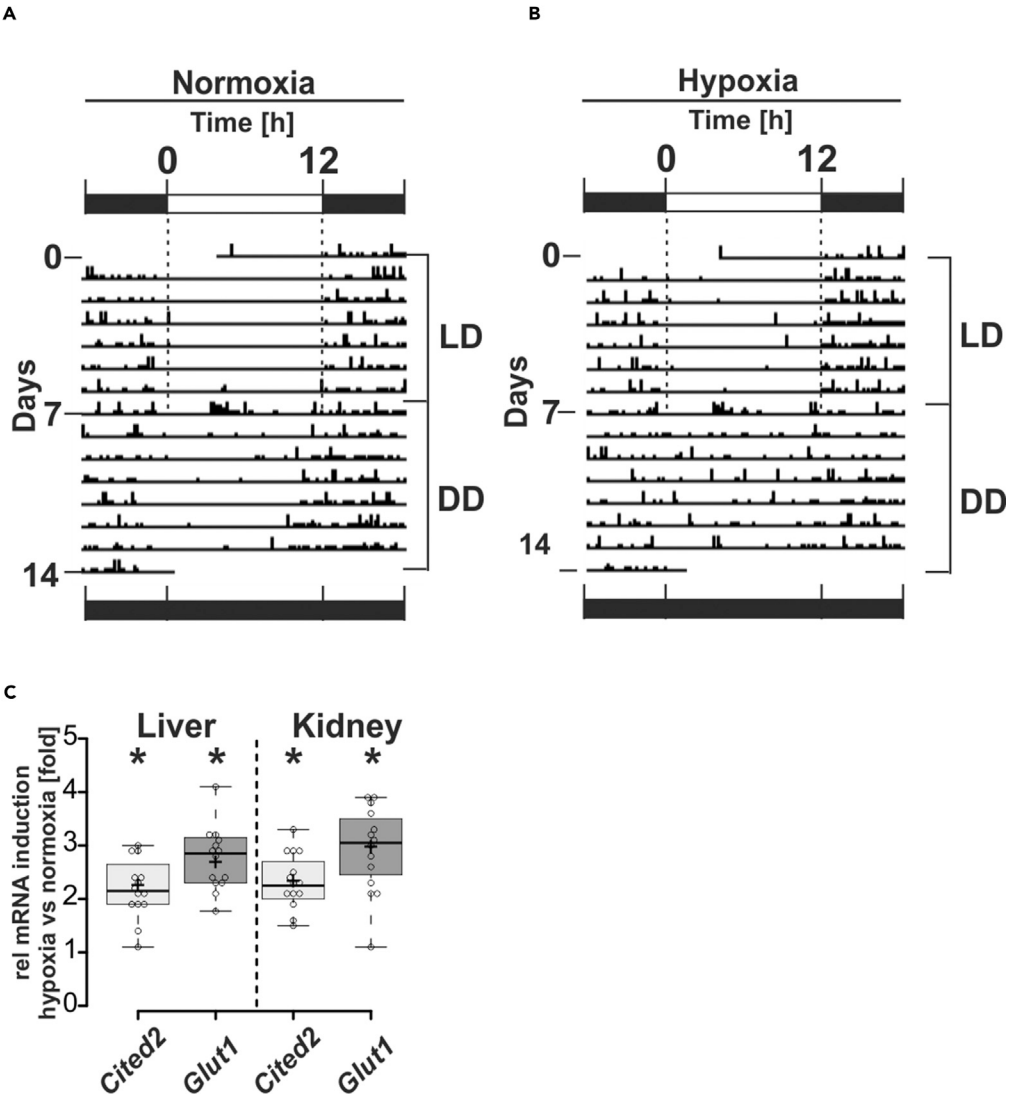

Figure 1. Representative Actograms of Individually Monitored Mice under Normoxia and Hypoxia at Light-Dark Cycles (LD) and Constant Darkness (DD)

(A) Mice were kept under normoxia (n = 14) and hypoxia (B) (n = 14) at 12-h light/12-h dark cycles (LD) for a week, which was followed by another week under the same conditions at constant darkness (DD).

(C) Hypoxia-dependent induction of *Cited2* and *Glut-1* mRNA in liver and kidney of the mice after the DD period. The respective mRNA levels were assessed by qRT-PCR, and the values indicate fold-change hypoxia versus normoxia. Boxes represent the interquartile range. Whiskers represent the minimum and maximum observations. *Significant difference normoxia versus hypoxia.

(PAI-1) fulfills these criteria and is well known to be a bona fide hypoxia-responsive and circadian-rhythm-regulated gene (Dimova et al., 2005; Kietzmann et al., 1999; Maemura et al., 2000; Schoenhard et al., 2003; Wang et al., 2006; Oishi et al., 2009; Cheng et al., 2011). Therefore we investigated whether the hypoxia-induced shifts in circadian rhythmicity are transferred to the expression of hypoxia-responsive target genes and to what extent one or the other response prevails. To examine this, we analyzed PAI-1 expression on protein and reporter gene level in synchronized cells. We found that hypoxia enhanced PAI-1 expression and shortened the circadian period of PAI-1 by about 40 min (Figures 3A–3D). Together, these data further substantiate that hypoxia and HIFs can advance the period of clock-dependent genes, whereas the amplitude is likely also modulated depending on the transcriptional context.

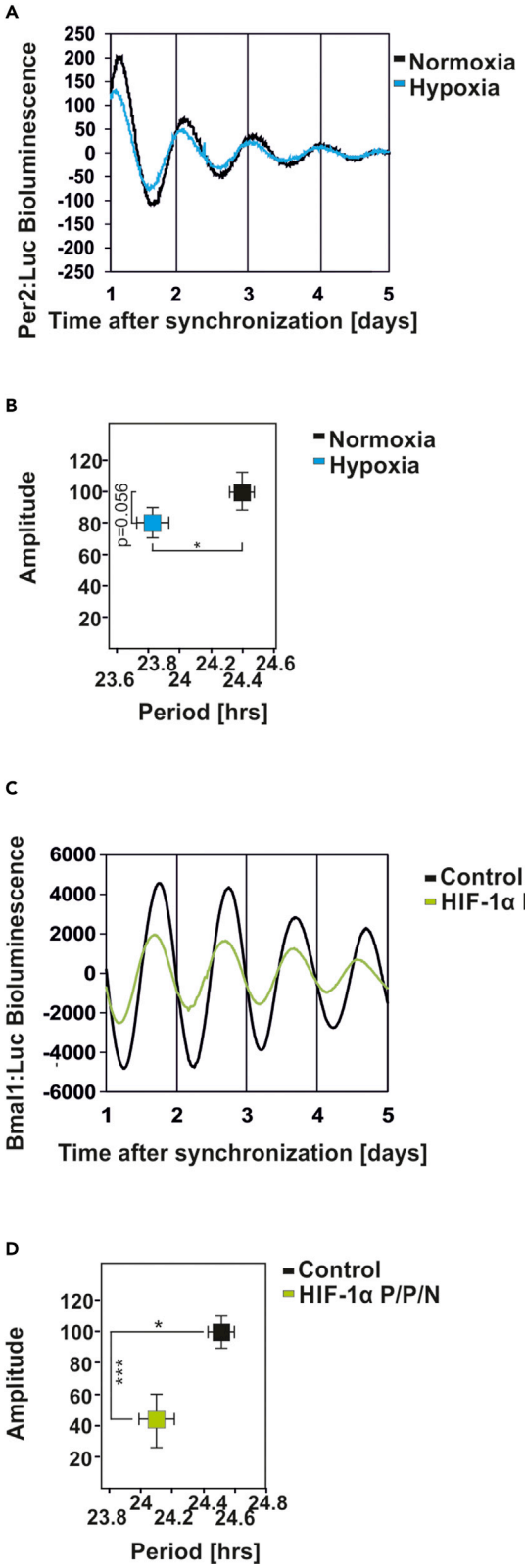
A
Per2:Luc Bioluminescence
250
200
150
100
50
0
-50
-100
-150
-200
-250
1
2
3
4
5
Time after synchronization [days]
Normoxia
Hypoxia
B
Amplitude
120
100
80
60
40
20
p=0.056
*
23.6
23.8
24
24.2
24.4
24.6
Period [hrs]
Normoxia
Hypoxia
C
Bmal1:Luc Bioluminescence
6000
4000
2000
0
-2000
-4000
-6000
1
2
3
4
5
Time after synchronization [days]
Control
HIF-1α P/P/N
D
Amplitude
120
100
80
60
40
20
*
***
23.8
24
24.2
24.4
24.6
24.8
Period [hrs]
Control
HIF-1α P/P/N

Figure 2. The Circadian Oscillation in NIH3T3 Cells Is Affected by HIF-1α

(A and B) (A) Representative examples of the bioluminescence oscillations in NIH3T3$^{mPer2:Luc}$ cells precultured under hypoxia (3% O_2) for 32 h. (B) Graphical illustration of the amplitude (y axis) and period length (x axis) upon hypoxia treatment. Data are mean ± SEM. *p < 0.05.

(C) Representative example of the bioluminescence oscillations in NIH3T3 cells cotransfected with an mBmal1:luciferase reporter construct and either empty vector (black line) or HIF-1α P/P/N (green line).

(D) Graphical illustration of the amplitude (y axis) and period length (x axis) upon overexpression of HIF-1α P/P/N. Data are mean ± SEM. *p < 0.05, ***p < 0.001.

CRY1 Interacts with HIF-1α and HIF-2α

Accumulating genetic data indicate that the negative limb of the circadian regulators, in particular CRY1, is responsible for maintaining the period length or amplitude of the circadian clock and that CRY1 is the most potent repressor in the clock's negative limb (Griffin et al., 1999; Kume et al., 1999; Van Der Horst et al., 1999; Vitaterna et al., 1999; Li et al., 2016; Liu et al., 2007; Khan et al., 2012; Matsuo et al., 2003; Koike et al., 2012; Langmesser et al., 2008; Ye et al., 2014; Michael et al., 2017). Based on CRY1's potency and responsibility for period and amplitude maintenance and the recent reports on the HIF-1α-BMAL1 cross talk (Wu et al., 2017; Peek et al., 2017) as well as the aforementioned findings that HIFs shortened the period and affected the amplitude of the circadian clock, we hypothesized that HIFs would interact with CRY1.

To examine this, we performed coimmunoprecipitation analyses with hypoxic mouse embryonic fibroblasts (MEFs). The assays revealed that CRY1 could be detected when HIF-1α was precipitated from the cells (Figure 4A). Furthermore, CRY1 could also be detected upon precipitation with HIF-2α antibodies, although the binding signal was low because of the low abundance of HIF-2α (Figure S2A). Next, we verified these interactions and performed western blot analyses from immunoprecipitates of HEK293 cells expressing Myc-tagged HIF-1α, V5-tagged HIF-2α, and hemagglutinin (HA)-tagged CRY1. The blots from anti-Myc-tagged HIF-1α or anti-V5-tagged HIF-2α immunoprecipitations showed the presence of HA-tagged CRY1 when probed with the HA-tag antibody indicating interaction of HIFα proteins and CRY1 (Figures 4B and S2B). In addition, HIFα proteins were also able to interact with CRY2 (Figures 4C and S2C). We also employed a bimolecular fluorescence complementation (BiFC) assay to verify whether these interactions are direct. The BiFC assay takes advantage from the possibility that a fluorescent protein complex can be formed through association of two per se non-interacting and non-fluorescent N-terminal (YN) and C-terminal (YC) fragments of the yellow fluorescent protein (YFP). The complementation of the fluorescent complex is achieved when YN and YC are brought into proximity owing to a direct interaction of the proteins fused to the YN and YC fragments (Figure 4D) (Kerppola, 2008). We generated vectors allowing expression of fusion proteins consisting of HIF-1α or HIF-2α and the C-terminal part of the YFP (HIF-1α-YC or HIF-2α -YC) as well as of CRY1 and the N-terminal part of the YFP (CRY1-YN). In addition, constructs for the HIFα partner ARNT as well as for the CRY1 partner PER1 served as positive controls to indicate HIF-1α -ARNT or CRY1-PER1 interaction, respectively. The BiFC analyses revealed a strong fluorescent signal when either HIF-1α-YC (Figures 4E and 4F) or HIF-2α-YC (Figure S2D) and CRY1-YN constructs were applied in the assay. In addition, a clear fluorescent signal could be observed when HIF-1α-YC was coexpressed with ARNT-YN or PER1-YC with CRY1-YN as positive controls (Figures 4E, S2D, and S2E). By contrast, when HIF-1α-YC or HIF-2α -YC was coexpressed with a vector encoding only YN (Figures 4E and 4F) no fluorescence was detected. Likewise, the coexpression of YC and YN did not result in the generation of fluorescence, indicating that the separated non-fluorescent fragments did not spontaneously self-assemble (Figures 4E and 4F). Together, these results indicate that HIF-1α and HIF-2α can interact with CRY1 in living cells.

The Tail Region of CRY-1 Interacts with HIF-1α

To find out which domain within CRY1 interacts with HIF-1α, we expressed Myc-tagged HIF1α along with different HA-tagged CRY1 protein variants in HEK293 cells (Figure 5A) and analyzed their interaction by coimmunoprecipitation experiments. Full-length CRY1 interacted with HIF-1α, but this interaction was lost when CRY1 proteins lacking either the CC and tail region or only the tail region were employed in the assays (Figure 5B). Thus, these data indicate that the tail region of CRY1 is necessary for the interaction of CRY1 with HIF-1α.

CRY1 Interacts with the bHLH Domain of HIF-1α

To map the exact HIF-1α domain that interacts with CRY1, we designed several Myc-tagged HIF-1α deletion mutants comprising one or several domains (Figure 6A) and performed coimmunoprecipitation

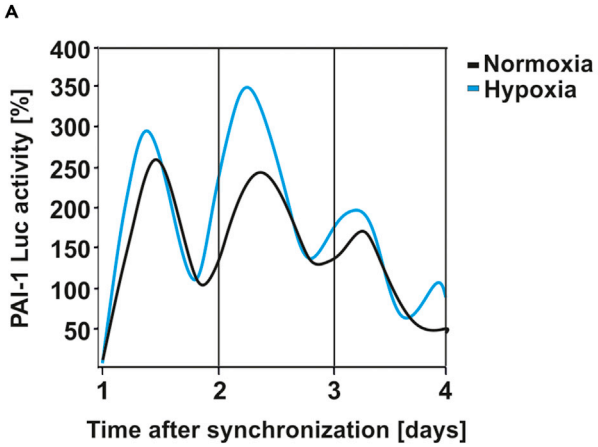
A
PAI-1 Luc activity [%]
400
350
300
250
200
150
100
50
1
2
3
4
Time after synchronization [days]
Normoxia
Hypoxia

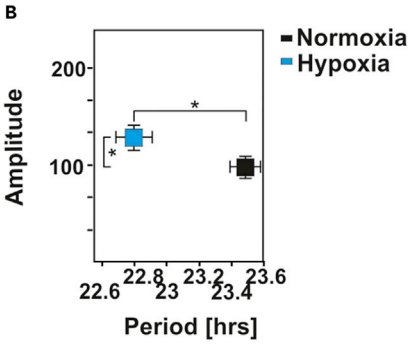
B
Amplitude
200
100
*
*
22.6
22.8
23
23.2
23.4
23.6
Period [hrs]
Normoxia
Hypoxia

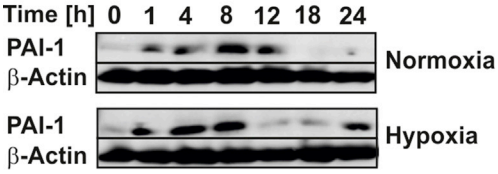
C
Time [h] 0 1 4 8 12 18 24
PAI-1
β-Actin
Normoxia
PAI-1
β-Actin
Hypoxia

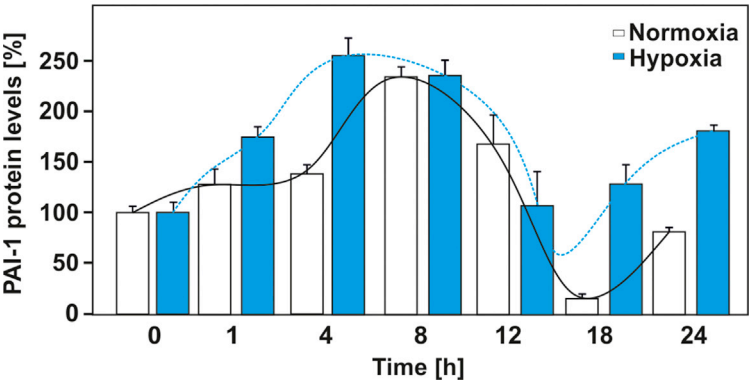
D
PAI-1 protein levels [%]
250
200
150
100
50
0
0
1
4
8
12
18
24
Time [h]
Normoxia
Hypoxia

Figure 3. The Circadian Oscillation of PAI-1 Expression Is Affected by Hypoxia

(A) Representative example of the bioluminescence oscillations in cells stably transfected with a PAI-1 promoter-driven luciferase construct under normoxia and hypoxia.

(B and C) (B) Graphical illustration of the amplitude (y axis) and period length (x axis) of PAI-1 promoter-driven luciferase expression under normoxia and hypoxia. Data are mean ± SEM. *$p < 0.05$. (C) Representative western blot analysis of total cell lysates of synchronized Rat-1 fibroblasts probed with PAI-1 and β-actin antibodies.

(D) Densitometric analysis of the PAI-1 protein levels presented on (C).

experiments in HA-CRY1 expressing HEK293 cells. When full-length HIF-1α or its deletion variants were pulled down with anti-Myc-tag antibodies we found that HA-CRY1 coprecipitated full-length HIF-1α and all deletion variants except the HIF-1α mutant lacking the bHLH domain (Figure 6B). Together, these results indicate that CRY1 interacts with the bHLH domain of HIF-1α.

CRY1 Inhibits Binding of HIF-1α to Its Target Gene Promoters

As CRY1 interacts with the HIF-1α bHLH domain, which primarily facilitates binding to DNA at target gene promoters, we next analyzed how CRY1 would affect hypoxia and HIF-dependent gene expression. First, we performed a series of functional reporter gene assays in HepG2 cells. Upon cotransfection of these cells with the hypoxia- and HIF-responsive wild-type (WT) human PAI-1 promoter Luc construct (pGL3-hPAI-806/+19) and an expression vector for CRY1 we found that the hypoxia-mediated increase in Luc activity was reduced in the presence of CRY1. This effect was mediated via the hypoxia responsive element (HRE) within the PAI-1 promoter because a construct with a mutated element (pGL3-hPAI-HREm) did not display this effect on Luc activity (Figure 7A). Vice versa, when we employed MEFs deficient for either CRY1 (ΔCRY1) or CRY2 (ΔCRY2) to measure PAI-1 expression, we found that deficiency of CRY1, but not CRY2, enhanced PAI-1 levels already under normoxia to almost the same levels as under hypoxia (Figures S3A and S3C). Reintroduction of CRY1 (Figures S3D and S3E) rescued the hypoxia-dependent PAI-1 expression indicating that these effects are largely CRY1 specific. In line with the interaction assays, these rescue effects were dependent on the tail region of CRY1 since only full-length CRY1, but not CRY1-Δtail, rescued the hypoxia-dependent induction of PAI-1 (Figures S3D and S3E). Thus, CRY1 appears to function as inhibitor of the hypoxia-dependent PAI-1 gene expression.

Next, we aimed to substantiate the inhibitory effect of CRY1 for HIF-driven genes and HIFs. To do this, we used bona fide hypoxia reporters containing either three WT HIF-binding HREs or three mutated HREs in front of the SV40 promoter and the luciferase gene. We then cotransfected these reporters together with a CRY1 expression vector or empty control vector into HepG2 cells. Hypoxia induced Luc activity in the control cells, whereas expression of CRY1 predominantly abolished Luc activity under hypoxia (Figure 7B). This effect was specific because mutation of critical nucleotides in the HRE (pGL3-HREm) abolished the induction of Luc activity under hypoxia and the repressive effect of CRY1 (Figure 7B).

As HIFs are dimers consisting of HIF-α and HIF-β (ARNT) subunits, we next investigated whether the CRY1 effect is primarily dependent on each subunit by using the pGL3-HRE Luc construct and the pGL3-HREm construct together with a CRY1 expression vector and HIF-1α, ARNT, or an empty control vector. We found that overexpression of CRY1 together with HIF-1α (Figure 7C) or HIF-2α (Figure S4), but not with ARNT, compromised the ability of HIF-1α to induce HRE-driven Luc activity. Furthermore, cotransfection of the Luc construct with mutant HREs (pGL3-HREm) along with the respective expression vectors alone or in combination resulted in Luc activities comparable with the control (Figure 7C). These results, together with the interaction data, suggest that CRY1 represses HIF-1α function.

To understand whether the inhibitory effect of CRY1 is accompanied by a reduced binding of HIF-1α to target gene promoters *in vivo*, we performed chromatin immunoprecipitation (ChIP) assays with WT MEFs or CRY1-deficient MEFs cultured under normoxia or hypoxia. The ChIP assays were performed with either unspecific IgG or specific antibodies against mouse HIF-1α or HIF-2α and PCR primers, which allowed amplification of the HIF-binding PAI-1, VEGF-A, PGK-1, and GLUT-1 promoters (Hu et al., 2007; Tanimoto et al., 2010; Wu et al., 2016; Schodel et al., 2011). The assays from WT MEFs reveal that both HIF-1α and HIF-2α preferentially associate with those promoter regions under hypoxia, whereas CRY1-deficient cells bound HIFs already under normoxia (Figures 7D and S5). Thereby, the normoxic binding of HIF-1α to each studied promoter in ΔCRY1 cells was already about 2- to 6-fold higher when compared with WT MEFs (Figure 7D). This binding was further increased in ΔCRY1 cells under hypoxia (Figures 7D

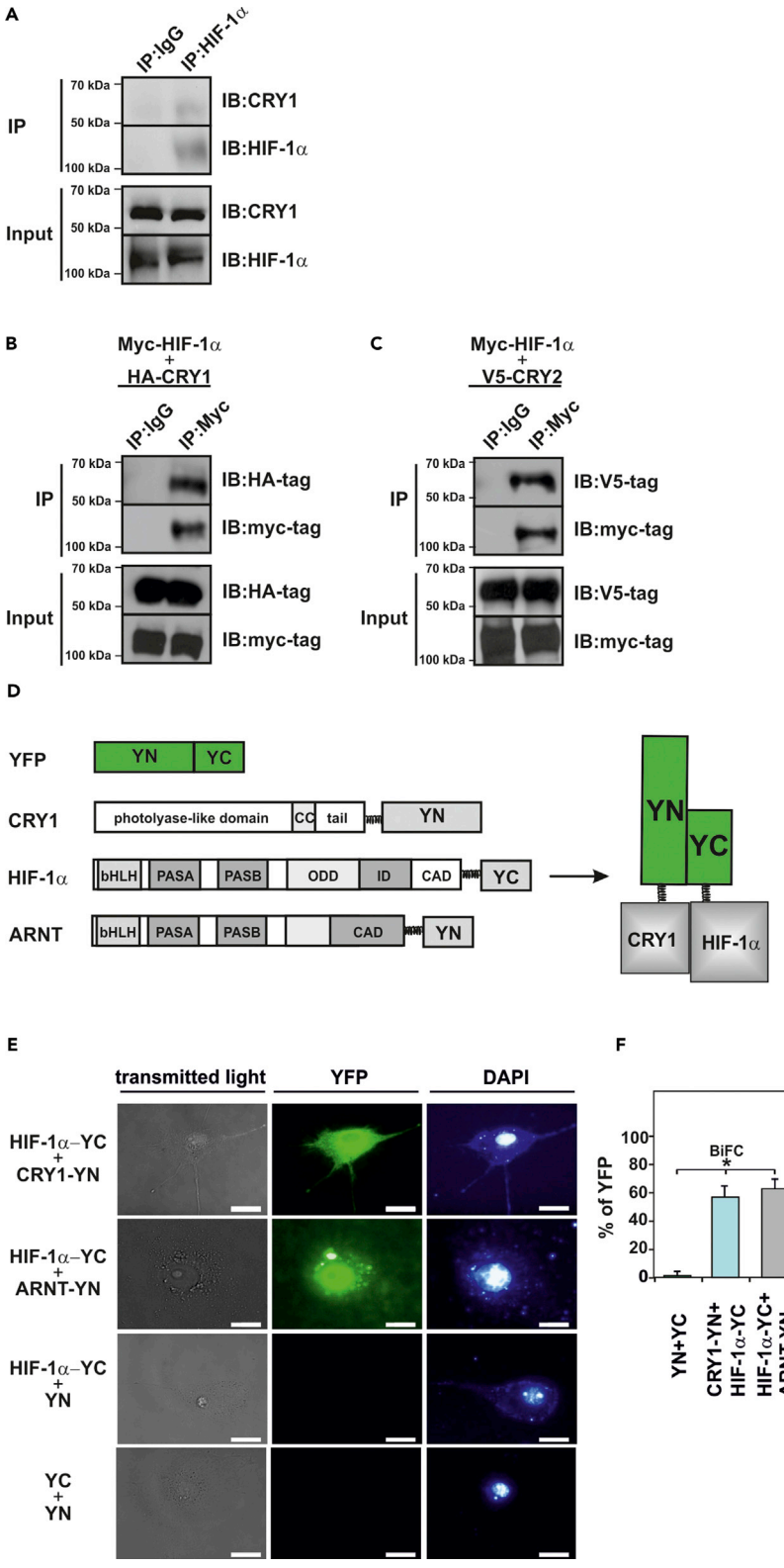
A
IP:IgG
IP:HIF-1α
IP
70 kDa
50 kDa
100 kDa
IB:CRY1
IB:HIF-1α
Input
70 kDa
50 kDa
100 kDa
IB:CRY1
IB:HIF-1α
B
Myc-HIF-1α
+
HA-CRY1
IP:IgG
IP:Myc
IP
70 kDa
50 kDa
100 kDa
IB:HA-tag
IB:myc-tag
Input
70 kDa
50 kDa
100 kDa
IB:HA-tag
IB:myc-tag
C
Myc-HIF-1α
+
V5-CRY2
IP:IgG
IP:Myc
IP
70 kDa
50 kDa
100 kDa
IB:V5-tag
IB:myc-tag
Input
70 kDa
50 kDa
100 kDa
IB:V5-tag
IB:myc-tag
D
YFP
YN
YC
CRY1
photolyase-like domain
CC
tail
YN
HIF-1α
bHLH
PASA
PASB
ODD
ID
CAD
YC
ARNT
bHLH
PASA
PASB
CAD
YN
YN
YC
CRY1
HIF-1α
E
transmitted light
YFP
DAPI
HIF-1α–YC
+
CRY1-YN
HIF-1α–YC
+
ARNT-YN
HIF-1α–YC
+
YN
YC
+
YN
F
% of YFP
100
80
60
40
20
0
BiFC
*
YN+YC
CRY1-YN+
HIF-1α-YC
HIF-1α-YC+
ARNT-YN
YFP

Figure 4. CRY1 Interacts with HIF-1α

(A) Coimmunoprecipitation (IP) assays from wild-type MEFs cultured under hypoxia in the presence of MG-132. Blots from anti-HIF-1α IPs were probed with the CRY1 and HIF-1α antibody. The blots shown are representative of three independent experiments. IB, immunoblotting.

(B and C) Coimmunoprecipitation studies with HEK293 cells, expressing myc-tagged HIF-1α with either (B) HA-tagged CRY1 or (C) V5-tagged CRY2. Blots from anti-myc-tag IPs were probed with HA-tag or V5-tag antibody. The blots shown are representative of three independent experiments.

(D and E) BiFC analysis. (D) Schematic representation of expressed proteins employed in BiFC. The sequences encoding amino acid residues 1–154 (N-terminus [YN]) or 155–238 (C-terminus [YC]) of the yellow fluorescent protein (YFP) were fused to the 3′ ends of the coding regions for HIF-1α, CRY1, or ARNT to generate HIF-1α -YC, CRY1-YN, and ARNT-YN, respectively. YN and YC are non-fluorescent fragments that do not interact per se with each other. An interaction between the proteins fused to the YN and YC fragments facilitates their association to form a bimolecular fluorescent complex. (E) Visualization of the BiFC signal by confocal microscopy. COS-7 cells cotransfected with the expression vectors for HIF-1α-YC, CRY1-YN, ARNT-YN, and vectors encoding only YN or YC were cultured on glass slides for 24 h. The fluorescence detection was performed using specific filter sets for YFP and DAPI. Scale bar, 10 μm.

(F) Quantification of the BiFC signal. Cells were transfected as in (E) and quantified by flow cytometry (cf. Transparent Methods). The cytomegalovirus promoter (CMV) driven-YFP signal was set to 100%. Data are mean ± SEM. *p < 0.05.

and S5). Together, these results indicate that the presence of CRY1 is able to reduce the binding of HIFs to the PAI-1, VEGF-A, PGK-1, and GLUT1 promoters.

Absence of CRY1 Increases HIF-1α Half-Life and Induces Its Transcription

Owing to the fact that CRY1 reduces binding of HIF-1α to its target gene promoters and that it is mainly regulated by post-translational stabilization, we hypothesized that CRY1 may promote HIF-1α degradation. To analyze this, we measured the HIF-1α protein half-life in the absence and presence of CRY1. Interestingly, we found that ΔCRY1 cells had higher HIF-1α protein levels than WT MEFs (Figure 8A). In addition, the CRY1-deficient cells displayed a prolonged HIF-1α half-life ($t_{1/2}$: 57 min versus ~45 min in WT cells) (Figures 8A and 8B). Furthermore, we examined whether lack of CRY1 would also affect HIF-1α mRNA levels. Concomitant with the increase in HIF-1α protein levels, we also found that the HIF-1α mRNA levels were increased by about 2-fold in the CRY1-deficient cells (Figure 8C). In addition, we found that the HIF-2α mRNA levels were induced by about 10-fold (Figure 8C). Overall, these data indicate that the CRY1-mediated functional repression of HIF-1α DNA binding is also accompanied by reduced transcription and enhanced HIF-1α protein degradation.

CRY1 and HIFs Have Opposite Roles in Cell Proliferation and Migration

The aforementioned findings suggest a reciprocal regulation of CRY1 and HIF-1α that would be of importance for cellular growth and survival, in particular during tumor development. To get an overview, we checked CRY1 and HIF-1α mRNA levels in cancer tissues and the corresponding normal tissues from the Oncomine (www.oncomine.org) database by applying a threshold of a >10-fold change and p value of 0.05. The results show that HIF-1α and CRY1 could be oppositely regulated in different tumor entities. In none of the cases HIF1α and CRY1 were regulated in the same manner, i.e., they were never together up- or downregulated in the same dataset. The reason(s) why HIF-1α expression was upregulated and CRY1 expression was not downregulated in the first and sixth microarray datasets and why HIF-1α expression was not upregulated and CRY1 was downregulated in the second and fifth microarray datasets are not known but may reflect the different status of tumor driving mutations, which certainly confound the regulation (Figure 9). Similarly, we observed CRY1 mRNA induction in HIF-1α-deficient cells (Figure S7). Given that HIF-1α overexpression is associated with poor survival in several patients with cancer (Semenza, 2017), these data together with the higher HIF-1α levels in ΔCRY1 cells imply that loss of CRY1 can promote cell growth. Indeed, we found that CRY1-deficient cells showed a higher rate in proliferation, migration, and colony formation than their WT counterparts (Figures 10B–10F and S6). To assess whether these functional differences are, at least in part, mediated by HIFs we re-investigated cellular proliferation, motility, and the ability to form colonies in CRY1-deficient cells with either CRISPR/Cas9-mediated HIF-1α deletion (Figure 10A) or short hairpin RNA (shRNA)-mediated knockdown of HIF-1α or HIF-2α (Figure S6). In contrast to CRY1 deficiency, lack of HIF-1α reduced proliferation (Figures 10B and 10C), motility (Figures 10E and 10F) and colony formation (Figure 10D). Interestingly, the ΔHIF-1α-ΔCRY1 cells harboring the combined knockout of HIF-1α and CRY1 displayed growth, motility, and colony-forming properties resembling those of WT cells (Figures 10B–10E). Similarly, we introduced scrambled non-effective shRNA or HIF-1α shRNA via retroviral infection into WT and ΔCRY1 cells. Again,

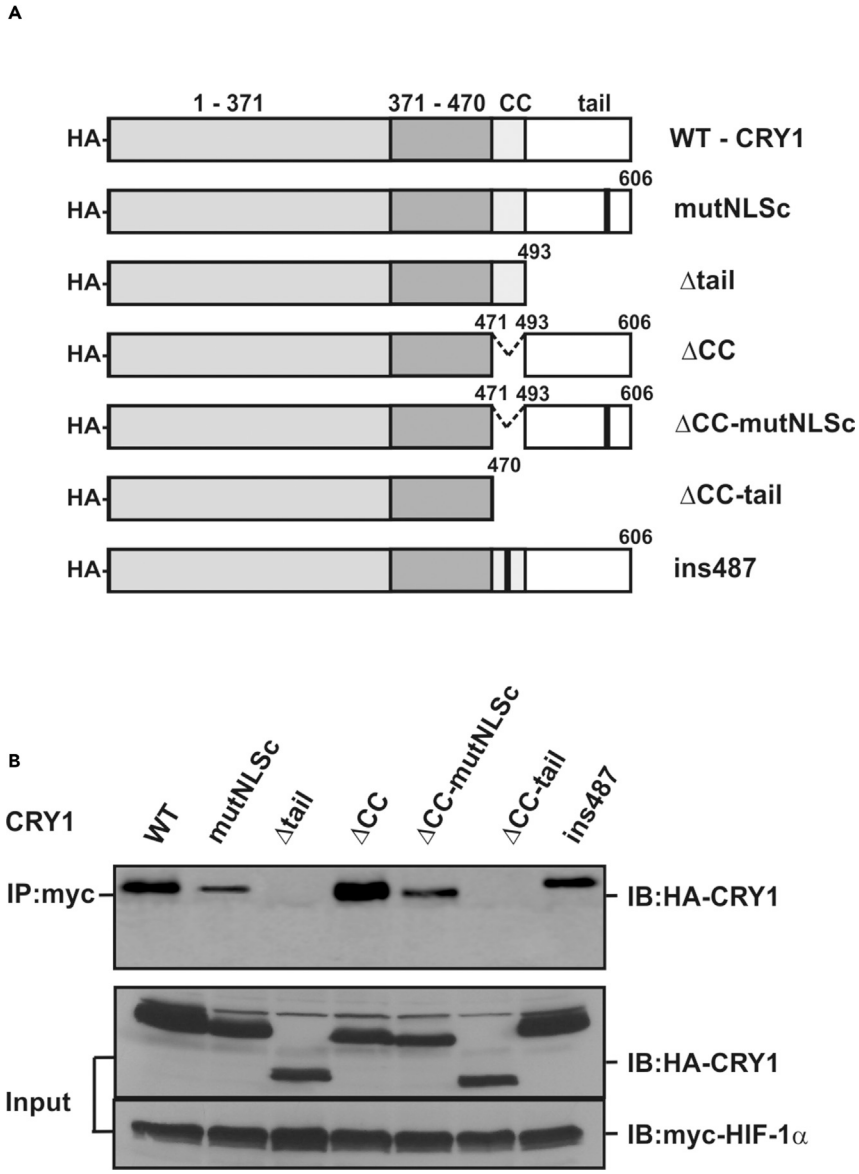

Figure 5. The Tail Domain of CRY1 Is Responsible for Interaction with HIF-1α

(A) Schematic representation of the HA-tagged CRY1 protein variants.

(B) HEK293 cells were transfected with myc-tagged HIF-1α together with HA-tagged full-length CRY1 or its mutants, cell extracts were prepared and immunoprecipitated with an anti-myc-tag antibody, and precipitates were analyzed by immunoblot with an anti-HA-tag antibody. As a control the expression levels of the CRY1 protein variants as well as myc-tagged HIF-1α were verified in whole-cell extracts (Input). IP, immunoprecipitation; IB, immunoblotting.

knockdown of HIF-1α or HIF-2α reduced the positive effects on migration and soft agar colony formation exerted by CRY1 deficiency alone (Figures S6A–S6C).

Thus concomitant deletion of HIFs in ΔCRY1 cells significantly reduced the stimulating effects exerted by the absence of CRY1 on cellular growth, colony formation, and cell migration. Together, these data indicate that CRY1 and HIFs have an opposite role on cellular growth.

DISCUSSION

The current study extends recently reported findings on the interplay between the circadian clock and the hypoxia pathway (Adamovich et al., 2017; Wu et al., 2017; Peek et al., 2017) by providing detailed

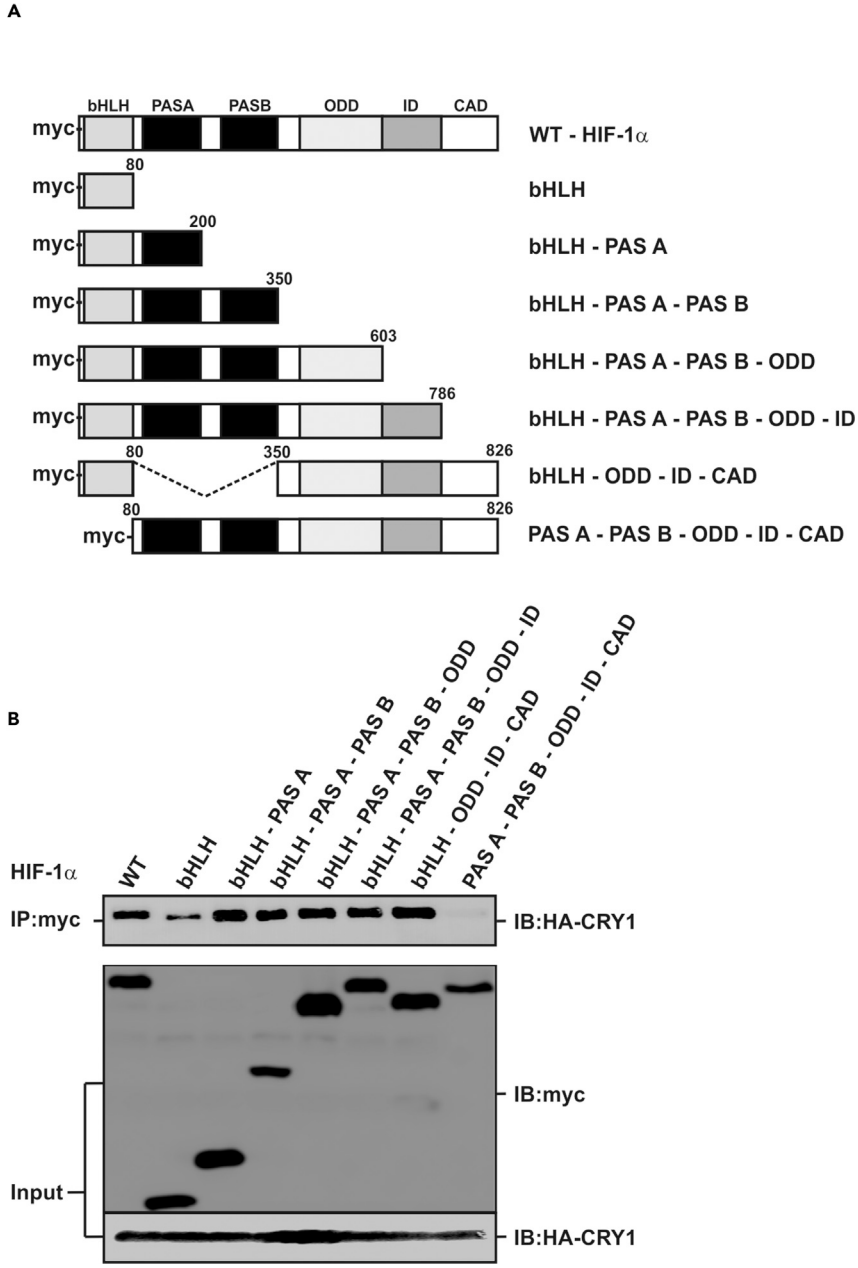

Figure 6. The bHLH Domain of HIF-1α Is Responsible for Interaction with CRY1

(A) Schematic representation of the myc-tagged HIF-1α protein variants.

(B) Coimmunoprecipitation experiments were performed with total proteins from HEK293 cells expressing HA-tagged CRY1 and myc-tagged full-length HIF-1α or its deletion variants. Anti-myc-tag antibody (IP, immunoprecipitation)-precipitated proteins were analyzed by immunoblot (IB, immunoblotting) using an anti-HA-tag antibody. As a control the expression levels of HIF-1α, its deletion variants, as well as the HA-tagged CRY1 proteins were verified in whole-cell extracts (Input).

mechanistic insights indicating how the circadian clock component CRY1 can regulate the hypoxia response pathway at the level of HIF-1α and HIF-2α. In particular we show that (1) CRY1 directly interacts with both HIF-1α and HIF-2α, (2) that the interaction of CRY1 with HIFs masks the DNA-binding domain of HIFs and consequently changes HIF DNA binding and expression of HIF target genes, and (3) that the CRY1-HIFα interaction is important for cellular growth.

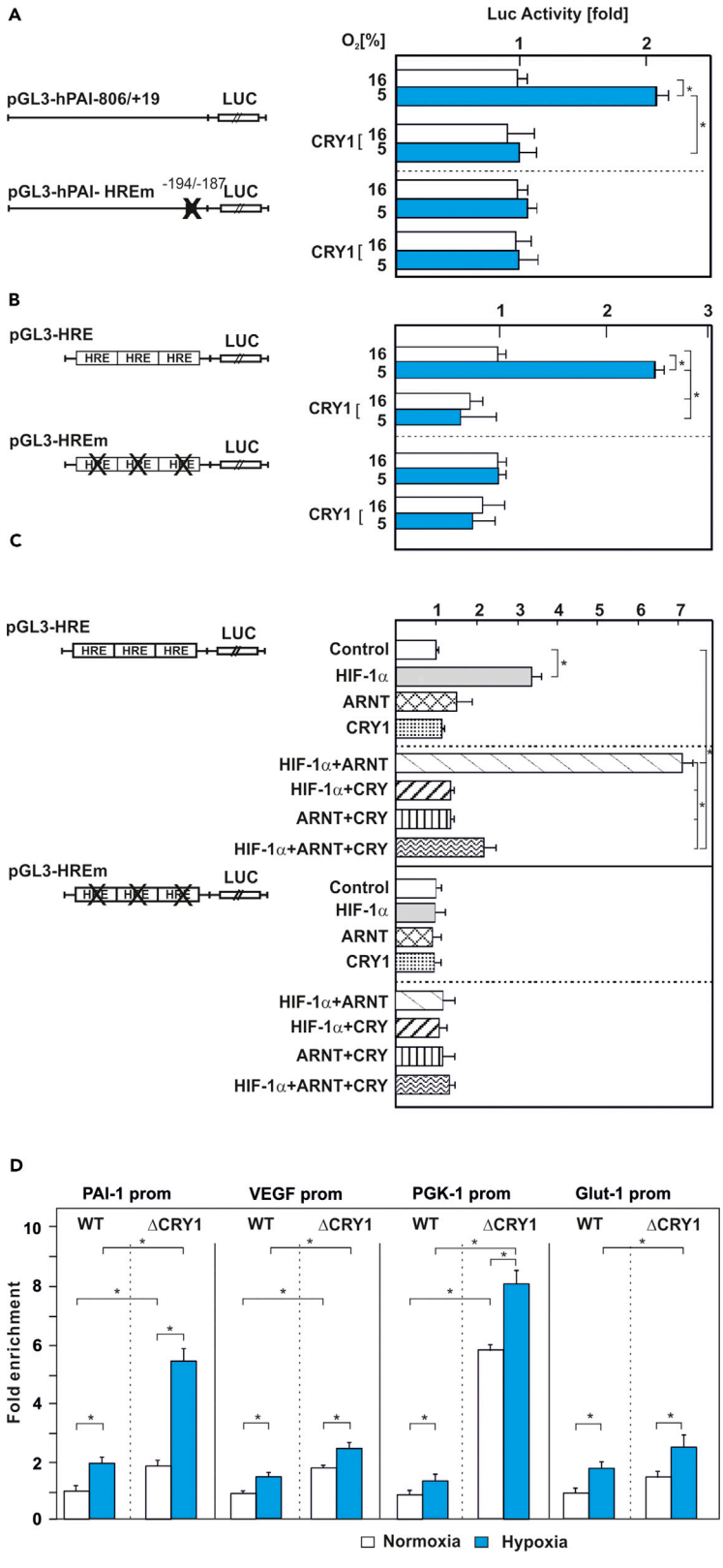
A
Luc Activity [fold]
O2[%]
pGL3-hPAI-806/+19
LUC
pGL3-hPAI- HREm
-194/-187
CRY1 [
B
pGL3-HRE
HRE
pGL3-HREm
C
Control
HIF-1α
ARNT
CRY1
HIF-1α+ARNT
HIF-1α+CRY
ARNT+CRY
HIF-1α+ARNT+CRY
D
PAI-1 prom
VEGF prom
PGK-1 prom
Glut-1 prom
WT
ΔCRY1
Fold enrichment
Normoxia
Hypoxia

Figure 7. CRY1 Inhibits Binding of HIF-1α to Its Target Gene Promoters

(A and B) Cells were cotransfected with an expression vector for CRY1 along with either (A) the wild-type human PAI-1 promoter Luc construct (pGL3-hPAI-806/+19) or a PAI-1 promoter with a mutated hypoxia-responsive element (HRE) (pGL3-hPAI-HREm) as well as with (B) Luc reporter gene constructs containing three HIF-binding HREs (pGL3-HRE) or three mutated HREs (pGL3-HREm) in front of the SV40 promoter and cultured under normoxia (16% O_2) and hypoxia (5% O_2) for 24 h. The Luc activity of pGL3-hPAI-806/+19-, pGL3-hPAI-HREm-, pGL3-HRE-, or pGL3-HREm-transfected cells at 16% O_2 was set to 1. Values are means ± SEM of at least three independent culture experiments, each performed in duplicate. Statistics, Student's t test for paired values: *significant difference, $p \leq 0.05$.

(C) Cells were cotransfected with pGL3-HRE or pGL3-HREm Luc reporter gene constructs and expression vectors encoding CRY1, HIF-1α, and ARNT alone or in combination. In each experiment the Luc activity of pGL3-HRE- or pGL3-HREm-transfected cells at 16% O_2 was set to 1. Values are means ± SEM of at least three independent culture experiments, each performed in duplicate. Statistics, Student's t test for paired values: *significant difference, $p \leq 0.05$.

(D) Chromatin immunoprecipitation (ChIP) was performed on cell lysates from formaldehyde cross-linked wild-type or CRY1-deficient MEFs, cultured under normoxia or hypoxia overnight. DNA fragments were co-precipitated with antibodies against mouse HIF-1α and amplified by quantitative PCR using primers specific for the mouse PAI-1, VEGF-A, PGK-1, and GLUT-1 promoters containing the corresponding HRE. Chromatin immunoprecipitation without antibody or using IgG instead of antibody served as additional specificity controls. Differences in the HIF-1α DNA-binding efficiency in wild-type and ΔCRY1 MEFs were calculated by the fold enrichment method relative to the IgG control. Values are means ± SEM of three independent experiments. Statistics, Student's t test for paired values: *significant difference, $p \leq 0.05$.

By broadening the knowledge about CRY1's involvement in more than the circadian clock pathway, the current study also extends the existing information about the interplay between the circadian clock and the hypoxia response pathway. Although this cross talk was proposed on the basis of *in vitro* findings almost 20 years ago (Hogenesch et al., 1998), a functional validation presenting a reciprocal regulation between the positive clock limb protein BMAL1 and HIF-1α (Peek et al., 2017) was just recently reported while this study on the negative limb was ongoing.

Our data show that hypoxia can modulate the circadian rhythm *in vivo* and *in vitro*. This is in line with findings of a recent study demonstrating that mimicry of circadian physiological oxygen rhythms as occurring in mouse blood can affect the setting of the clock (Adamovich et al., 2017). In addition, we show that mice under chronic hypoxia become arrhythmic in total darkness (DD) indicating more severe effects of hypoxia on the clock in general (Figure 1). Although the reasons are not known yet, these activity data may be the result of a partial uncoupling of central and peripheral clocks due to disturbed adaptation to chronic hypoxia similar to that seen with restricted feeding (Damiola et al., 2000). This may express as arrhythmicity in periods coinciding with an increased oxygen consumption (Adamovich et al., 2017) such as the onset of activity and food ingestion, which in mice normally occur during the dark phase of the daily rhythm.

A complimentary approach with Per2:Luc cells exposed to hypoxia as well as with mBmal1:Luc circadian reporter cells in which we overexpressed variants of HIF-1α and HIF-2α revealed that hypoxia and HIFs can not only shorten the period but also decrease the amplitude of the clock (Figures 2 and S1). The amplitude effects of the HIFs seen here are in line with previous studies in which C2C12 and U2OS cells were treated with DMOG (Wu et al., 2017; Peek et al., 2017). Interestingly, our data appeared to be in contrast to one study (Wu et al., 2017) wherein overexpression of a degradation-resistant HIF1α (HIF1α-P402A/P564A) resulted in a lengthening of the period of up to 4 h in U2OS cells. The reasons for the discrepancies might be multiple and could be attributable to the different model systems used (U2OS osteosarcoma cells there versus non-cancer mammalian fibroblasts in our study) or the different way of cell synchronization (dexamethasone versus forskolin in our study). In addition, the other study used the doxycycline-dependent tetR system to overexpress HIF-1α in U2OS cells. Hence, secondary effects of the doxycycline treatment, which are known to inhibit protein translation in mitochondria and to impair metabolism may lead to effects that can confound experimental results (Moullan et al., 2015; Chatzispyrou et al., 2015). Nonetheless, and despite the differences, both studies underline the important roles of HIF-1α as circadian modulator.

Although no study, including the present, can yet explain the detailed mechanism by which HIFs and DMOG affect the period, it is tempting to speculate that this may be mediated by the proposed effects of HIF on BMAL1 (Peek et al., 2017). Indeed, deletion of HIF-1α resulted in a dramatic reduction in BMAL1 mRNA levels (Figure S7) in line with another study wherein overexpression of HIF-1α induced it (Yu et al., 2015). However, HIFs and DMOG appear to act by a different mechanism when seeing the effects

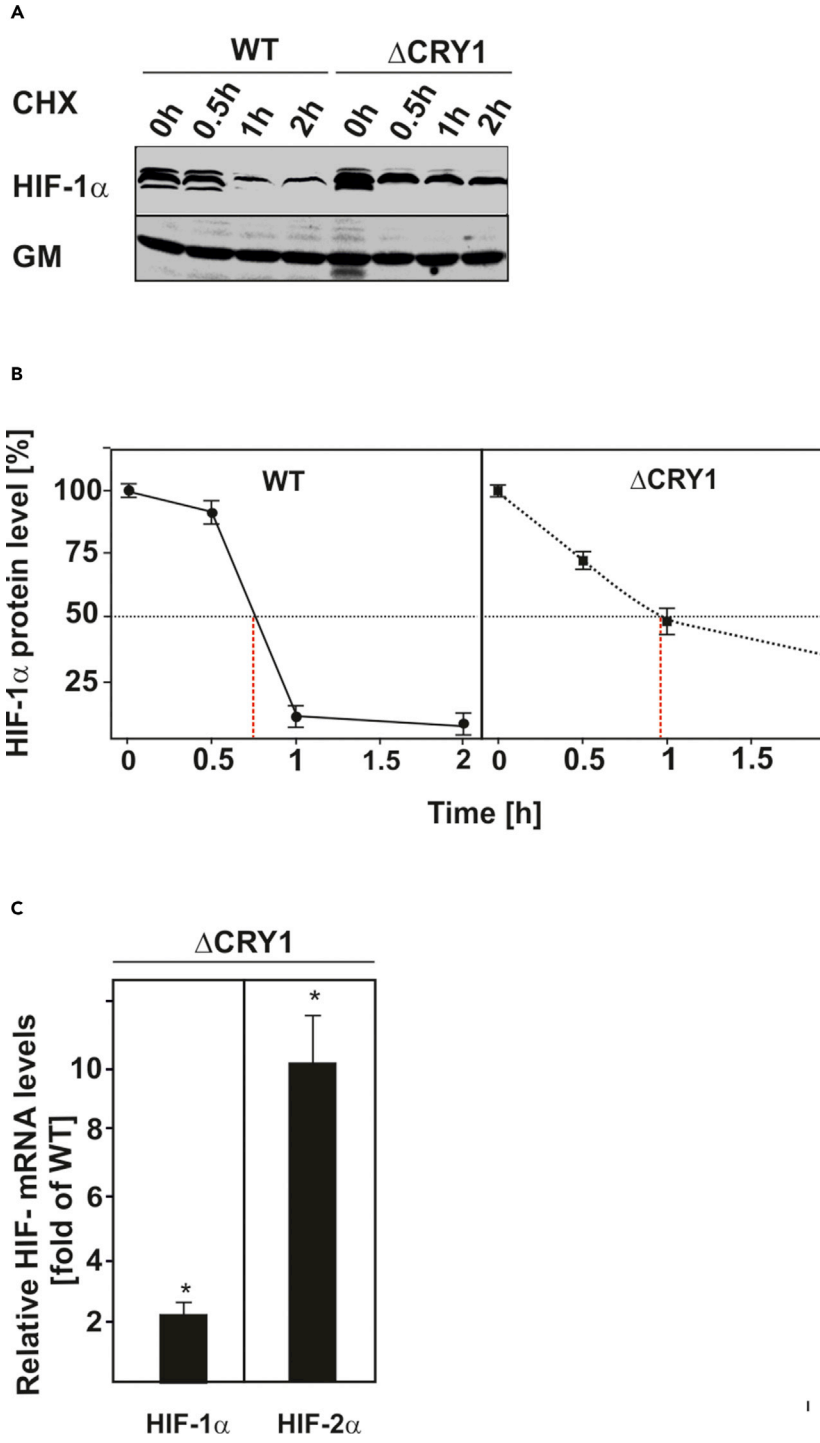

Figure 8. CRY1 Deficiency Increases HIF-1α Protein Half-Life and Transcription

(A and B) Measurement of HIF-1α protein half-life in wild-type (WT) and CRY-deficient MEFs (ΔCRY1). Cells were cultured for 4 h under hypoxia (5% O_2) and after inhibition of protein synthesis with cycloheximide (CHX; 10 μg/mL), endogenous HIF-1α protein levels were determined by western blot analysis with an antibody against mouse HIF-1α. Autoradiographic signals were obtained by chemiluminescence and quantified. Values are means ± SEM of three independent experiments. (A) Representative western blots. (B) Quantification of HIF-1α half-life.

Figure 8. *Continued*

(C) Quantitative qRT-PCR data. The values in wild-type MEFs (WT) were set to 1. Values represent means ± SEM of at least three independent experiments. Statistics, Student's t test for paired values: *significant difference WT versus CRY1-deficient cells; $p \leq 0.05$.

on the period. In the present and previous studies (Wu et al., 2017; Peek et al., 2017) DMOG lengthened the period (Figure S1), whereas overexpression of HIFs shortened it (Figures 2 and S1). The difference in period length between DMOG and HIFs is explainable by the rather pleiotropic effects of DMOG, which is a synthetic analog of α-ketoglutarate/2-oxoglutarate. As such, DMOG can act as a pan-inhibitor of α-ketoglutarate/2-oxoglutarate-dependent dioxygenases, a family consisting of about ~70 enzymes in humans, among them the HIF-prolyl 4-hydroxylases (Hirsila et al., 2003; Kietzmann et al., 2017). Consequently, a number of HIF-independent effects may influence the data achieved upon usage of DMOG. In line are the results obtained upon knockdown of the α-ketoglutarate/2-oxoglutarate-dependent dioxygenases FIH-1 and the EglN family, which also resulted in a lengthened period (Wu et al., 2017). To circumvent the pleiotropic DMOG effects, we used a hydroxylation-resistant HIF-1α variant (PPN) to specify whether it can mimic the shorter period as seen during chronic hypoxia. Importantly, both HIF-1α and HIF-2α could resemble the effects of hypoxia on the period (Figures 2 and S1). Thus the difference in period length upon DMOG usage or EglN and FIH-1 knockdown versus hypoxia or HIF overexpression as seen in this study can be attributed to non-HIF targets of which several, so far unknown, may be involved in clock regulation (Ivan and Kaelin, 2017). Together, all these data suggest that the hypoxia-signaling pathway may have different layers that can affect the circadian period and amplitude.

Intrigued by the HIF effects on the circadian period, and given that CRY proteins represent dominant critical regulators of the circadian period length in humans and mice (Van Der Horst et al., 1999; Vitaterna et al., 1999; Li et al., 2016; Hirota et al., 2012; Ode et al., 2017; Oshima et al., 2015; Siepka et al., 2007; Patke et al., 2017) we hypothesized a connection between HIFs and CRYs. Therefore, we probed whether CRY1 and CRY2 can interact with HIF-1α and HIF-2α, and indeed our experiments revealed that both CRY proteins were able to undergo interaction with the two HIF proteins (Figures 4 and S2).

The CRY1 protein contains a conserved photolyase homology region crucially involved in repression of CLOCK/BMAL1; a C-terminal helix also known as the predicted coiled coil (CC), which interacts with PER2 and FBXL3 in a mutually exclusive manner; and a C-terminal extension also referred to as the "tail" (Figure 5) (Chaves et al., 2011; Merbitz-Zahradnik and Wolf, 2015). Our mapping experiments showed that HIF-1α interacts with the CRY1 "tail" region, a part of the protein (Figure 5), which has the ability to modulate the period length and amplitude of the resulting oscillation (Khan et al., 2012; Xu et al., 2015). In line, a recent report showed that a dominant CRY1 allele coding for a protein with a deletion of 24 residues in the tail region (Patke et al., 2017) caused lengthening of the circadian period and could be linked to familial delayed sleep phase disorder. Thus the effects seen under hypoxia on the period length are in accord with the interaction of HIF-1α with CRY1's tail region. Furthermore, the tail has been shown to affect CRY1 translocation, to interact with the BMAL1 transactivation domain possibly in an acetylation-dependent fashion, and to be phosphorylated in a manner that involves regulation by DNA-PK (Xu et al., 2015; Chaves et al., 2006; Czarna et al., 2011; Hirayama et al., 2007). In addition, the existence of a nuclear localization signal in the CRY1 tail coincides well with the nuclear localization of its interaction with HIFs as seen in the BiFC assays (Figures 4 and S2). In line, the bHLH domain of HIF-1α, which appears to work as the CRY1 interaction module (Figure 6), also contains a nuclear localization sequence (Kallio et al., 1998). Although not directly tested in this study, a similar mode of interaction is likely occurring with HIF-2α because both share an amino acid sequence identity of ~85% in the bHLH domain.

As the HIF bHLH domain is primarily involved in DNA binding, it is conceivable that the CRY1 tail could affect binding of HIFs to target gene promoters causing a repression of their expression. Thereby the repressive effect of CRY1 may not only depend solely on HIF-1α but also on the promoter context. This is exemplified with the PAI-1 promoter where CRY1 did not repress its activity under normoxia, whereas it clearly suppressed its hypoxia-dependent induction. To minimize the influence of the promoter context and to generalize the findings with respect to HIFs, we then used a bona fide hypoxia reporter containing three HREs as enhancers in front of the SV40 promoter and the luciferase gene. Indeed, these HRE reporter gene assays revealed that CRY1 suppressed their activity under normoxia and their hypoxia and HIF-1-dependent induction. Vice versa, the ChIP experiments from CRY1-deficient cells showed enhanced binding of HIFs to target gene promoters under both normoxia and hypoxia (Figures 7D and S5). Together,

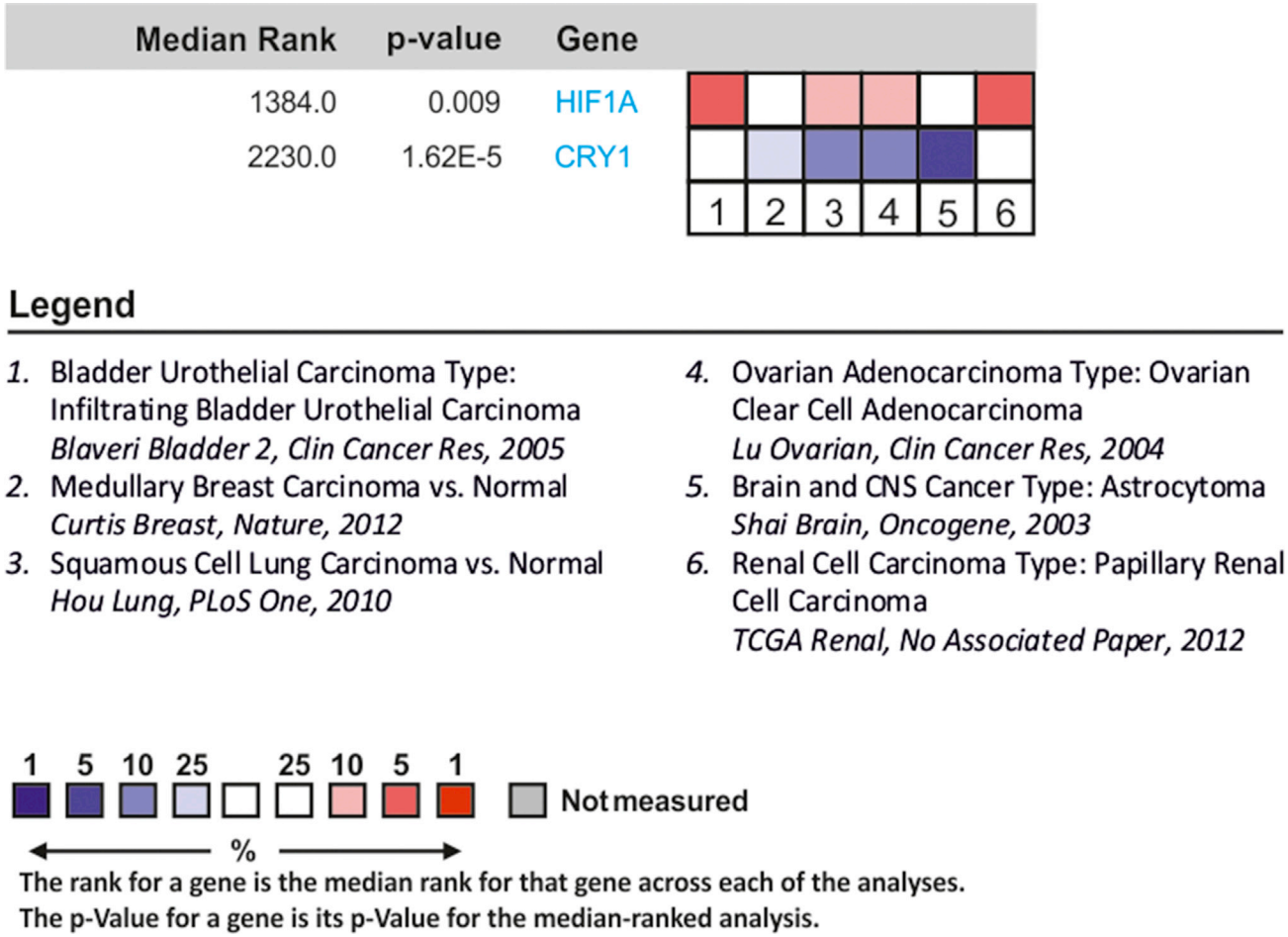

Figure 9. CRY-1 and HIF-1α Show an Opposite Expression Pattern in Human Cancer Cohorts

Analysis of CRY1 and HIF1A mRNA expression profiles in the Oncomine database. Six microarray datasets from different cancer entities were analyzed for CRY1 and HIF1A mRNA expression and compared with normal tissue using a threshold of >10-fold change and a p value <0.05. Red, upregulated in cancer versus normal tissue; blue, downregulated in cancer versus normal tissue. Data are presented as log2 median-centered intensity with the median rank of CRY1 and HIF1A mRNA through each dataset analysis. The rank for a gene is the median rank for that gene across each of the analyses. The p value for a gene is its p value for the median-ranked analysis.

these effects need to be seen in context with our data showing that absence of CRY1 regulates HIF-1α at two levels, namely, by increasing its transcription and its stability (Figure 8). Consequently, the net effect is an increase in HIF-1α binding to its enhancers under both conditions. Overall, these data point to a suppressive role of CRY1, and in particular its tail, in the transcriptional response toward hypoxia at various stages of the circadian cycle.

The current data are also in agreement with another recent study also showing enhanced HIF-1α levels in CRY-deficient cells, whereas BMAL1 absence decreased HIF-1α levels (Peek et al., 2017). Similarly, Per2 supported recruitment of HIF-1α to the VEGF promoter (Kobayashi et al., 2017). Together with reports from mouse liver and cardiac tissue, showing that *Hif1α* mRNA levels cycled in a circadian manner (Eckle et al., 2012; Wu et al., 2017) and data showing a rhythmic appearance of nuclear HIF1α in mouse brain and kidney (Adamovich et al., 2017), the current findings substantiate the existence of a feedback mechanism in which the circadian clock pathway can regulate HIF-1α expression.

Earlier findings from different cancer entities such as chronic myeloid leukemia (Yang et al., 2011), B cell chronic lymphocytic leukemia (Jantus Lewintre et al., 2009), prostate cancer (Zhu et al., 2009), epithelial ovarian cancer (Tokunaga et al., 2008), and colon cancer (Mazzoccoli et al., 2016; Huisman et al., 2016)

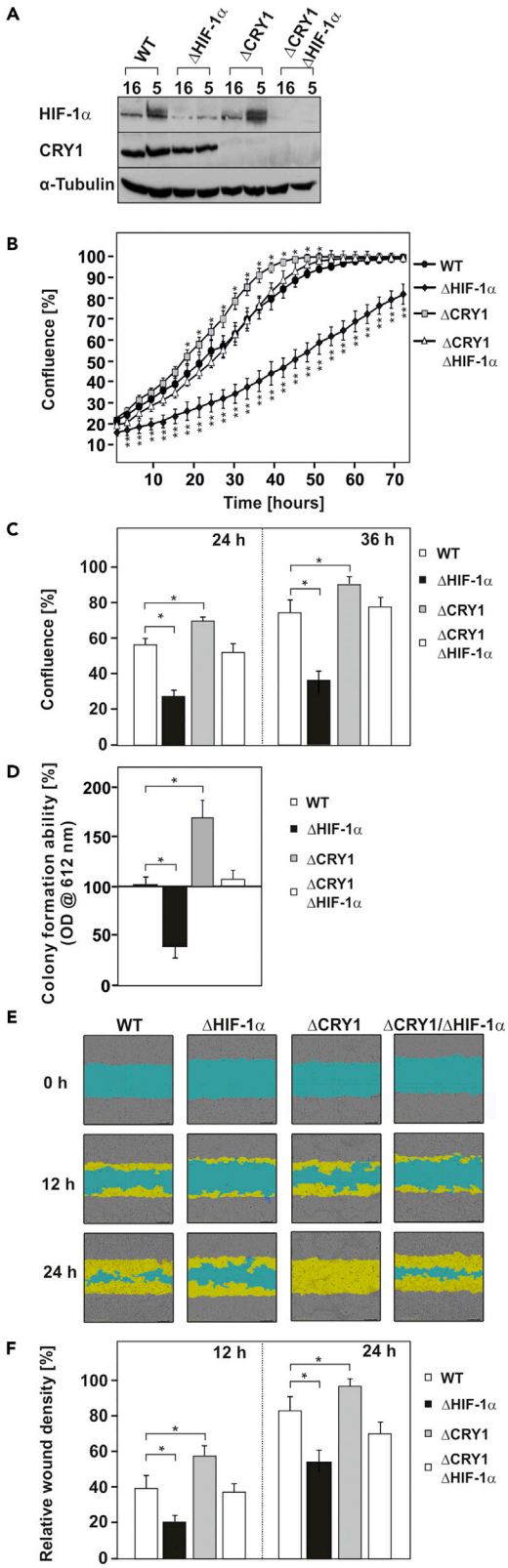
A
WT
ΔHIF-1α
ΔCRY1
ΔCRY1 ΔHIF-1α
16 5 16 5 16 5 16 5
HIF-1α
CRY1
α-Tubulin
B
Confluence [%]
Time [hours]
WT
ΔHIF-1α
ΔCRY1
ΔCRY1 ΔHIF-1α
C
24 h
36 h
Confluence [%]
D
Colony formation ability [%] (OD @ 612 nm)
E
WT
ΔHIF-1α
ΔCRY1
ΔCRY1/ΔHIF-1α
0 h
12 h
24 h
F
12 h
24 h
Relative wound density [%]

Figure 10. CRY-1 and HIF-1α Show an Opposite Role on Cell Proliferation and Migration

(A) Representative HIF-1α western blots in WT MEFs, ΔCRY1, ΔHIF-1α, and ΔCRY1/ΔHIF-1α MEFs.

(B) Proliferation rate of WT, ΔCRY1, ΔHIF-1α, and ΔCRY1/ΔHIF-1α cells quantified by dynamic imaging using percentage of confluence at 3-h time intervals.

(C) Chart of 24- and 36-h time points. Statistics, Student's t test for paired values: *significant difference, $p \leq 0.01$.

(D) Quantification of the colony formation ability of WT, ΔCRY1, ΔHIF-1α, and ΔCRY1/ΔHIF-1α cells as measured by soft agar assay. The cells were plated in soft agar and allowed to grow for 2 weeks under hypoxia. Cell growth was measured using Resazurin staining in a microplate reader with an excitation wavelength of 584 nm and emission at 612 nm. The OD_{612} in WT MEFs was set to 100%. Statistics, Student's t test for paired values: *significant difference, $p < 0.05$.

(E) Representative images of the wound recovery of WT, ΔCRY1, ΔHIF-1α, and ΔCRY1/ΔHIF-1α cells at 0, 12, and 24 h after introduction of the wound. Scale bar, 300 μm.

(F) Chart of 12- and 24-h time points. Statistics, Student's t test for paired values: *significant difference, $p < 0.01$.

indicate a reduced CRY1 expression and associated this, as well as a deregulation in *Bmal1* or *Per2* expression (Huisman et al., 2016), to be a negative prognostic marker.

Vice versa, HIFs are frequently found to be enriched in the hypoxic areas of solid tumors (Talks et al., 2000; Zhong et al., 1998). By showing that CRY1 deficiency induces HIF levels (Figures 10 and S6) and accelerates proliferation and migration, two key aspects relevant to carcinogenesis, and that knocking out HIFs either by CRISPR/Cas9 or by the use of shRNAs reversed these effects, our study now provides a mechanistic link between the above-mentioned genetic association studies.

Although these findings underline the connection between CRY1 and HIFs, it appears that other regulators involved in carcinogenesis can also be regulated by CRY1. For example, several findings from both *Per* and *Cry* knockout mice strongly suggest that their dysfunction cooperates with loss of *p53* during carcinogenesis (Fu and Kettner, 2013). This is also in agreement with studies showing the complex interconnections between the individual components of the circadian clock with nucleotide excision repair and DNA damage in mice (Kang and Sancar, 2009; Kang et al., 2009) which affect not only carcinogenesis but also aging.

In summary, the current study presents a mechanistic link by which the lack of circadian control at the CRY1 level can favor the action of HIFs during cellular growth, which underpins that chronic misalignment between our lifestyle and the rhythm dictated by our endogenous circadian clock is associated with an increased risk for various diseases including cancer.

Limitations of the Study

In this study we made use of mice and MEFs to investigate the cross talk between HIFs and CRY1. Although this study provided novel insights into how CRY1 affects the HIF system in MEFs, subsequent studies are necessary to investigate the implication for cancer cells and cancer treatment. It is likely, however, that other circadian proteins (such as tCK2) could contribute to the regulation as well. As different regulators may affect CRY1 expression and activity in different ways, their exact roles and contributions need to be further studied.

METHODS

All methods can be found in the accompanying Transparent Methods supplemental file.

SUPPLEMENTAL INFORMATION

Supplemental Information can be found online at https://doi.org/10.1016/j.isci.2019.02.027.

ACKNOWLEDGMENTS

This work was supported by grants from the Finnish Academy of Science (SA 296027), Jane and Aatos Erkko Foundation, the Finnish Cancer Foundation, the Finnish Center of International Mobility (CIMO), Biocenter Oulu, and University of Oulu to T.K.

AUTHOR CONTRIBUTIONS

Conceptualization, T.K. and E.Y.D.; Methodology, E.Y.D., M.J., K.K., D.M., T.F.C., F.T., M.O., J.H., N.B., K.A.M., K.-H.H., P.K., I.C., G.v.d.H., and T.K.; Investigation, E.Y.D., M.J., K.K., D.M., T.F.C., F.T., M.O., J.H., N.B., K.A.M., I.C.; Data Curation, E.Y.D., M.J., K.K., D.M., T.F.C., F.T., M.O., J.H., N.B., and K.A.M.;

Visualization, E.Y.D., M.J., K.K., D.M., T.F.C., M.O., I.C., G.v.d.H., and T.K.; Writing – Original Draft, E.Y.D., M.J., G.v.d.H., and T.K.; Writing – Review & Editing, E.Y.D., I.C., G.v.d.H., and T.K.; Funding Acquisition, G.v.d.H., P.K., and T.K.; Resources, G.v.d.H., P.K., K.-H.H., and T.K..; Supervision, E.Y.D., and T.K.

DECLARATION OF INTERESTS

The authors declare no competing interests.

Received: March 6, 2018
Revised: January 3, 2019
Accepted: February 22, 2019
Published: March 29, 2019

REFERENCES

Adamovich, Y., Ladeuix, B., Golik, M., Koeners, M.P., and Asher, G. (2017). Rhythmic oxygen levels reset circadian clocks through HIF1a. Cell Metab. *25*, 93–101.

Albrecht, U. (2012). Timing to perfection: the biology of central and peripheral circadian clocks. Neuron *74*, 246–260.

Asher, G., and Schibler, U. (2011). Crosstalk between components of circadian and metabolic cycles in mammals. Cell Metab. *13*, 125–137.

Balsalobre, A., Damiola, F., and Schibler, U. (1998). A serum shock induces circadian gene expression in mammalian tissue culture cells. Cell *93*, 929–937.

Chatzispyrou, I.A., Held, N.M., Mouchiroud, L., Auwerx, J., and Houtkooper, R.H. (2015). Tetracycline antibiotics impair mitochondrial function and its experimental use confounds research. Cancer Res. *75*, 4446–4449.

Chaves, I., Pokorny, R., Byrdin, M., Hoang, N., Ritz, T., Brettel, K., Essen, L., Van Der Horst, G.T.J., Batschauer, A., and Ahmad, M. (2011). The cryptochromes: blue light photoreceptors in plants and animals. Annu. Rev. Plant Biol. *62*, 335–364.

Chaves, I., Yagita, K., Barnhoorn, S., Okamura, H., Van Der Horst, G.T.J., and Tamanini, F. (2006). Functional evolution of the photolyase/cryptochrome protein family: importance of the C terminus of mammalian CRY1 for circadian core oscillator performance. Mol. Cell. Biol. *26*, 1743–1753.

Cheng, S., Jiang, Z., Zou, Y., Chen, C., Wang, Y., Liu, Y., Xiao, J., Guo, H., and Wang, Z. (2011). Downregulation of Clock in circulatory system leads to an enhancement of fibrinolysis in mice. Exp. Biol. Med. (Maywood) *236*, 1078–1084.

Chilov, D., Hofer, T., Bauer, C., Wenger, R.H., and Gassmann, M. (2001). Hypoxia affects expression of circadian genes PER1 and CLOCK in mouse brain. FASEB J. *15*, 2613–2622.

Czarna, A., Breitkreuz, H., Mahrenholz, C.C., Arens, J., Strauss, H.M., and Wolf, E. (2011). Quantitative analyses of cryptochrome-mBMAL1 interactions: mechanistic insights into the transcriptional regulation of the mammalian circadian clock. J. Biol. Chem. *286*, 22414–22425.

Damiola, F., Le Minli, N., Preitner, N., Kornmann, B., Fleury-Olela, F., and Schibler, U. (2000). Restricted feeding uncouples circadian oscillators in peripheral tissues from the central pacemaker in the suprachiasmatic nucleus. Genes Dev. *14*, 2950–2961.

Dimova, E.Y., Moller, U., Herzig, S., Fink, T., Zachar, V., Ebbesen, P., and Kietzmann, T. (2005). Transcriptional regulation of plasminogen activator inhibitor-1 expression by insulin-like growth factor-1 via MAP kinases and hypoxia-inducible factor-1 in HepG2 cells. Thromb. Haemost. *93*, 1176–1184.

Eckle, T., Hartmann, K., Bonney, S., Reithel, S., Mittelbronn, M., Walker, L.A., Lowes, B.D., Han, J., Borchers, C.H., Buttrick, P.M., et al. (2012). Adora2b-elicited Per2 stabilization promotes a HIF-dependent metabolic switch crucial for myocardial adaptation to ischemia. Nat. Med. *18*, 774–782.

Filipski, E., and Levi, F. (2009). Circadian disruption in experimental cancer processes. Integr. Cancer Ther. *8*, 298–302.

Flügel, D., Görlach, A., and Kietzmann, T. (2012). GSK-3beta regulates cell growth, migration, and angiogenesis via Fbw7 and USP28-dependent degradation of HIF-1alpha. Blood *119*, 1292–1301.

Fu, L., and Kettner, N.M. (2013). The circadian clock in cancer development and therapy. Prog. Mol. Biol. Transl. Sci. *119*, 221–282.

Fu, L., and Lee, C.C. (2003). The circadian clock: pacemaker and tumour suppressor. Nat. Rev. Cancer *3*, 350–361.

Griffin, E.A., Jr., Staknis, D., and Weitz, C.J. (1999). Light-independent role of CRY1 and CRY2 in the mammalian circadian clock. Science *286*, 768–771.

Hirayama, J., Sahar, S., Grimaldi, B., Tamaru, T., Takamatsu, K., Nakahata, Y., and Sassone-Corsi, P. (2007). CLOCK-mediated acetylation of BMAL1 controls circadian function. Nature *450*, 1086–1090.

Hirota, T., Lee, J.W., St. John, P.C., Sawa, M., Iwaisako, K., Noguchi, T., Pongsawakul, P.Y., Sonntag, T., Welsh, D.K., Brenner, D.A., et al. (2012). Identification of small molecule activators of cryptochrome. Science *337*, 1094–1097.

Hirsila, M., Koivunen, P., Gunzler, V., Kivirikko, K.I., and Myllyharju, J. (2003). Characterization of the human prolyl 4-hydroxylases that modify the hypoxia-inducible factor. J. Biol. Chem. *278*, 30772–30780.

Hogenesch, J.B., Gu, Y.Z., Jain, S., and Bradfield, C.A. (1998). The basic-helix-loop-helix-PAS orphan MOP3 forms transcriptionally active complexes with circadian and hypoxia factors. Proc. Natl. Acad. Sci. U S A *95*, 5474–5479.

Hu, C.J., Sataur, A., Wang, L., Chen, H., and Simon, M.C. (2007). The N-terminal transactivation domain confers target gene specificity of hypoxia-inducible factors HIF-1alpha and HIF-2alpha. Mol. Biol. Cell *18*, 4528–4542.

Huisman, S.A., Ahmadi, A.R., IJzermans, J.N., Verhoef, C., van der Horst, G.T., and de Bruin, R.W. (2016). Disruption of clock gene expression in human colorectal liver metastases. Tumour Biol. *37*, 13973–13981.

Ivan, M., and Kaelin, W.G., Jr. (2017). The EGLN-HIF O2-sensing system: multiple inputs and feedbacks. Mol. Cell *66*, 772–779.

Jantus Lewintre, E., Reinoso Martin, C., Montaner, D., Marin, M., Jose Terol, M., Farras, R., Benet, I., Calvete, J.J., Dopazo, J., and Garcia-Conde, J. (2009). Analysis of chronic lymphotic leukemia transcriptomic profile: differences between molecular subgroups. Leuk. Lymphoma *50*, 68–79.

Kaelin, W.G., Jr., and Ratcliffe, P.J. (2008). Oxygen sensing by metazoans: the central role of the HIF hydroxylase pathway. Mol. Cell *30*, 393–402.

Kallio, P.J., Okamoto, K., O'Brien, S., Carrero, P., Makino, Y., Tanaka, H., and Poellinger, L. (1998). Signal transduction in hypoxic cells: inducible nuclear translocation and recruitment of the CBP/p300 coactivator by the hypoxia-inducible factor-1alpha. EMBO J. *17*, 6573–6586.

Kang, T.H., Reardon, J.T., Kemp, M., and Sancar, A. (2009). Orcadian oscillation of nucleotide excision repair in mammalian brain. Proc. Natl. Acad. Sci. U S A *106*, 2864–2867.

Kang, T., and Sancar, A. (2009). Circadian regulation of DNA excision repair: implications for chrono-chemotherapy. Cell Cycle *8*, 1665–1667.

Kerppola, T.K. (2008). Bimolecular fluorescence complementation (BiFC) analysis as a probe of protein interactions in living cells. Annu. Rev. Biophys. *37*, 465–487.

Khan, S.K., Xu, H., Ukai-Tadenuma, M., Burton, B., Wang, Y., Ueda, H.R., and Liu, A.C. (2012). Identification of a novel cryptochrome differentiating domain required for feedback repression in circadian clock function. J. Biol. Chem. *287*, 25917–25926.

Kietzmann, T., Petry, A., Shvetsova, A., Gerhold, J.M., and Gorlach, A. (2017). The epigenetic landscape related to reactive oxygen species formation in the cardiovascular system. Br. J. Pharmacol. *174*, 1533–1554.

Kietzmann, T., Roth, U., and Jungermann, K. (1999). Induction of the plasminogen activator inhibitor-1 gene expression by mild hypoxia via a hypoxia response element binding the hypoxia-inducible factor-1 in rat hepatocytes. Blood *94*, 4177–4185.

Ko, C.H., and Takahashi, J.S. (2006). Molecular components of the mammalian circadian clock. Hum. Mol. Genet. *15* (*Suppl. 2*), R271–R277.

Kobayashi, M., Morinibu, A., Koyasu, S., Goto, Y., Hiraoka, M., and Harada, H. (2017). A circadian clock gene, PER2, activates HIF-1 as an effector molecule for recruitment of HIF-1alpha to promoter regions of its downstream genes. FEBS J. *284*, 3804–3816.

Koike, N., Yoo, S.H., Huang, H.C., Kumar, V., Lee, C., Kim, T.K., and Takahashi, J.S. (2012). Transcriptional architecture and chromatin landscape of the core circadian clock in mammals. Science *338*, 349–354.

Kume, K., Zylka, M.J., Sriram, S., Shearman, L.P., Weaver, D.R., Jin, X., Maywood, E.S., Hastings, M.H., and Reppert, S.M. (1999). mCRY1 and mCRY2 are essential components of the negative limb of the circadian clock feedback loop. Cell *98*, 193–205.

Langmesser, S., Tallone, T., Bordon, A., Rusconi, S., and Albrecht, U. (2008). Interaction of circadian clock proteins PER2 and CRY with BMAL1 and CLOCK. BMC Mol. Biol. *9*, 41.

Li, Y., Xiong, W., and Zhang, E.E. (2016). The ratio of intracellular CRY proteins determines the clock period length. Biochem. Biophys. Res. Commun. *472*, 531–538.

Liu, A.C., Welsh, D.K., Ko, C.H., Tran, H.G., Zhang, E.E., Priest, A.A., Buhr, E.D., Singer, O., Meeker, K., Verma, I.M., et al. (2007). Intercellular coupling confers robustness against mutations in the SCN circadian clock network. Cell *129*, 605–616.

Maemura, K., de la Monte, S.M., Chin, M.T., Layne, M.D., Hsieh, C.M., Yet, S.F., Perrella, M.A., and Lee, M.E. (2000). CLIF, a novel cycle-like factor, regulates the circadian oscillation of plasminogen activator inhibitor-1 gene expression. J. Biol. Chem. *275*, 36847–36851.

Masson, N., and Ratcliffe, P.J. (2014). Hypoxia signaling pathways in cancer metabolism: the importance of co-selecting interconnected physiological pathways. Cancer Metab. *2*, 3.

Matsuo, T., Yamaguchi, S., Mitsui, S., Emi, A., Shimoda, F., and Okamura, H. (2003). Control mechanism of the circadian clock for timing of cell division in vivo. Science *302*, 255–259.

Mazzoccoli, G., Colangelo, T., Panza, A., Rubino, R., De Cata, A., Tiberio, C., Valvano, M.R., Pazienza, V., Merla, G., Augello, B., et al. (2016). Deregulated expression of cryptochrome genes in human colorectal cancer. Mol. Cancer *15*, 6.

Merbitz-Zahradnik, T., and Wolf, E. (2015). How is the inner circadian clock controlled by interactive clock proteins?: structural analysis of clock proteins elucidates their physiological role. FEBS Lett. *589*, 1516–1529.

Michael, A.K., Fribourgh, J.L., Chelliah, Y., Sandate, C.R., Hura, G.L., Schneidman-Duhovny, D., Tripathi, S.M., Takahashi, J.S., and Partch, C.L. (2017). Formation of a repressive complex in the mammalian circadian clock is mediated by the secondary pocket of CRY1. Proc. Natl. Acad. Sci. U S A *114*, 1560–1565.

Moullan, N., Mouchiroud, L., Wang, X., Ryu, D., Williams, E.G., Mottis, A., Jovaisaite, V., Frochaux, M.V., Quiros, P.M., Deplancke, B., et al. (2015). Tetracyclines disturb mitochondrial function across eukaryotic models: a call for caution in biomedical research. Cell Rep. *10*, 1681–1691.

Ode, K.L., Ukai, H., Susaki, E.A., Narumi, R., Matsumoto, K., Hara, J., Koide, N., Abe, T., Kanemaki, M.T., Kiyonari, H., and Ueda, H.R. (2017). Knockout-rescue embryonic stem cell-derived mouse reveals circadian-period control by quality and quantity of CRY1. Mol. Cell *65*, 176–190.

Oishi, K., Miyazaki, K., Uchida, D., Ohkura, N., Wakabayashi, M., Doi, R., Matsuda, J., and Ishida, N. (2009). PERIOD2 is a circadian negative regulator of PAI-1 gene expression in mice. J. Mol. Cell. Cardiol. *46*, 545–552.

Oshima, T., Yamanaka, I., Kumar, A., Yamaguchi, J., Nishiwaki-Ohkawa, T., Muto, K., Kawamura, R., Hirota, T., Yagita, K., Irle, S., et al. (2015). C-H activation generates period-shortening molecules that target cryptochrome in the mammalian circadian clock. Angew. Chem. Int. Ed. *54*, 7193–7197.

Patke, A., Murphy, P.J., Onat, O.E., Krieger, A.C., Özçelik, T., Campbell, S.S., and Young, M.W. (2017). Mutation of the human circadian clock gene CRY1 in familial delayed sleep phase disorder. Cell *169*, 203–215.e13.

Peek, C.B., Levine, D.C., Cedernaes, J., Taguchi, A., Kobayashi, Y., Tsai, S.J., Bonar, N.A., McNulty, M.R., Ramsey, K.M., and Bass, J. (2017). Circadian clock interaction with HIF1a mediates oxygenic metabolism and anaerobic glycolysis in skeletal muscle. Cell Metab. *25*, 86–92.

Rana, S., and Mahmood, S. (2010). Circadian rhythm and its role in malignancy. J. Circadian Rhythms *8*, 3.

Richards, J., and Gumz, M.L. (2012). Advances in understanding the peripheral circadian clocks. FASEB J. *26*, 3602–3613.

Sahar, S., and Sassone-Corsi, P. (2009). Metabolism and cancer: the circadian clock connection. Nat. Rev. Cancer *9*, 886–896.

Sato, T.K., Yamada, R.G., Ukai, H., Baggs, J.E., Miraglia, L.J., Kobayashi, T.J., Welsh, D.K., Kay, S.A., Ueda, H.R., and Hogenesch, J.B. (2006). Feedback repression is required for mammalian circadian clock function. Nat. Genet. *38*, 312–319.

Schodel, J., Oikonomopoulos, S., Ragoussis, J., Pugh, C.W., Ratcliffe, P.J., and Mole, D.R. (2011). High-resolution genome-wide mapping of HIF-binding sites by ChIP-seq. Blood *117*, e207–e217.

Schoenhard, J.A., Smith, L.H., Painter, C.A., Eren, M., Johnson, C.H., and Vaughan, D.E. (2003). Regulation of the PAI-1 promoter by circadian clock components: differential activation by BMAL1 and BMAL2. J. Mol. Cell. Cardiol. *35*, 473–481.

Semenza, G.L. (2017). Hypoxia-inducible factors: coupling glucose metabolism and redox regulation with induction of the breast cancer stem cell phenotype. EMBO J. *36*, 252–259.

Shostak, A. (2017). Circadian clock, cell division, and cancer: from molecules to organism. Int. J. Mol. Sci. *18*, https://doi.org/10.3390/ijms18040873.

Siepka, S.M., Yoo, S.H., Park, J., Song, W., Kumar, V., Hu, Y., Lee, C., and Takahashi, J.S. (2007). Circadian mutant overtime reveals F-box protein FBXL3 regulation of cryptochrome and period gene expression. Cell *129*, 1011–1023.

Straif, K., Baan, R., Grosse, Y., Secretan, B., Ghissassi, F.E., Bouvard, V., Altieri, A., Benbrahim-Tallaa, L., and Cogliano, V.; WHO International Agency for Research on Cancer Monograph Working Group (2007). Carcinogenicity of shift-work, painting, and fire-fighting. Lancet Oncol. *8*, 1065–1066.

Talks, K.L., Turley, H., Gatter, K.C., Maxwell, P.H., Pugh, C.W., Ratcliffe, P.J., and Harris, A.L. (2000). The expression and distribution of the hypoxia-inducible factors HIF-1alpha and HIF-2alpha in normal human tissues, cancers, and tumor-associated macrophages. Am. J. Pathol. *157*, 411–421.

Tanimoto, K., Tsuchihara, K., Kanai, A., Arauchi, T., Esumi, H., Suzuki, Y., and Sugano, S. (2010). Genome-wide identification and annotation of HIF-1alpha binding sites in two cell lines using massively parallel sequencing. Hugo J. *4*, 35–48.

Tokunaga, H., Takebayashi, Y., Utsunomiya, H., Akahira, J., Higashimoto, M., Mashiko, M., Ito, K., Niikura, H., Takenoshita, S., and Yaegashi, N. (2008). Clinicopathological significance of circadian rhythm-related gene expression levels in patients with epithelial ovarian cancer. Acta Obstet. Gynecol. Scand. *87*, 1060–1070.

Van Der Horst, G.T.J., Muijtjens, M., Kobayashi, K., Takano, R., Kanno, S., Takao, M., De Wit, J., Verkerk, A., Eker, A.P.M., Van Leenen, D., et al. (1999). Mammalian Cry1 and Cry2 are essential for maintenance of circadian rhythms. Nature *398*, 627–630.

Vitaterna, M.H., Selby, C.P., Todo, T., Niwa, H., Thompson, C., Fruechte, E.M., Hitomi, K., Thresher, R.J., Ishikawa, T., Miyazaki, J., et al. (1999). Differential regulation of mammalian period genes and circadian rhythmicity by cryptochromes 1 and 2. Proc. Natl. Acad. Sci. U S A *96*, 12114–12119.

Wang, J., Yin, L., and Lazar, M.A. (2006). The orphan nuclear receptor Rev-erb alpha regulates circadian expression of plasminogen activator inhibitor type 1. J. Biol. Chem. *281*, 33842–33848.

Wu, H.T., Kuo, Y.C., Hung, J.J., Huang, C.H., Chen, W.Y., Chou, T.Y., Chen, Y., Chen, Y.J., Chen, Y.J., Cheng, W.C., et al. (2016). K63-polyubiquitinated HAUSP deubiquitinates HIF-1alpha and dictates H3K56 acetylation promoting hypoxia-induced tumour progression. Nat. Commun. *7*, 13644.

Wu, Y., Tang, D., Liu, N., Xiong, W., Huang, H., Li, Y., Ma, Z., Zhao, H., Chen, P., Qi, X., and Zhang, E.E. (2017). Reciprocal regulation between the circadian clock and hypoxia signaling at the genome level in mammals. Cell Metab. *25*, 73–85.

Xu, H., Gustafson, C.L., Sammons, P.J., Khan, S.K., Parsley, N.C., Ramanathan, C., Lee, H.-., Liu, A.C., and Partch, C.L. (2015). Cryptochrome 1 regulates the circadian clock through dynamic interactions with the BMAL1 C terminus. Nat. Struct. Mol. Biol. *22*, 476–484.

Yagita, K., Tamanini, F., Van der Horst, G.T.J., and Okamura, H. (2001). Molecular mechanisms of the biological clock in cultured fibroblasts. Science *292*, 278–281.

Yang, M.Y., Yang, W.C., Lin, P.M., Hsu, J.F., Hsiao, H.H., Liu, Y.C., Tsai, H.J., Chang, C.S., and Lin, S.F. (2011). Altered expression of circadian clock genes in human chronic myeloid leukemia. J. Biol. Rhythms *26*, 136–148.

Ye, R., Selby, C.P., Chiou, Y.Y., Ozkan-Dagliyan, I., Gaddameedhi, S., and Sancar, A. (2014). Dual modes of CLOCK: BMAL1 inhibition mediated by Cryptochrome and period proteins in the mammalian circadian clock. Genes Dev. *28*, 1989–1998.

Yoo, S.H., Ko, C.H., Lowrey, P.L., Buhr, E.D., Song, E.J., Chang, S., Yoo, O.J., Yamazaki, S., Lee, C., and Takahashi, J.S. (2005). A noncanonical E-box enhancer drives mouse Period2 circadian oscillations in vivo. Proc. Natl. Acad. Sci. U S A *102*, 2608–2613.

Yu, C., Yang, S.L., Fang, X., Jiang, J.X., Sun, C.Y., and Huang, T. (2015). Hypoxia disrupts the expression levels of circadian rhythm genes in hepatocellular carcinoma. Mol. Med. Rep. *11*, 4002–4008.

Zhong, H., Agani, F., Baccala, A.A., Laughner, E., Rioseco-Camacho, N., Isaacs, W.B., Simons, J.W., and Semenza, G.L. (1998). Increased expression of hypoxia inducible factor-1alpha in rat and human prostate cancer. Cancer Res. *58*, 5280–5284.

Zhu, Y., Stevens, R.G., Hoffman, A.E., Fitzgerald, L.M., Kwon, E.M., Ostrander, E.A., Davis, S., Zheng, T., and Stanford, J.L. (2009). Testing the circadian gene hypothesis in prostate cancer: a population-based case-control study. Cancer Res. *69*, 9315–9322.

ISCI, Volume *13*

Supplemental Information

The Circadian Clock Protein CRY1

Is a Negative Regulator of HIF-1α

Elitsa Y. Dimova, Mirza Jakupovic, Kateryna Kubaichuk, Daniela Mennerich, Tabughang Franklin Chi, Filippo Tamanini, Małgorzata Oklejewicz, Jens Hänig, Nadiya Byts, Kari A. Mäkelä, Karl-Heinz Herzig, Peppi Koivunen, Ines Chaves, Gijsbertus van der Horst, and Thomas Kietzmann

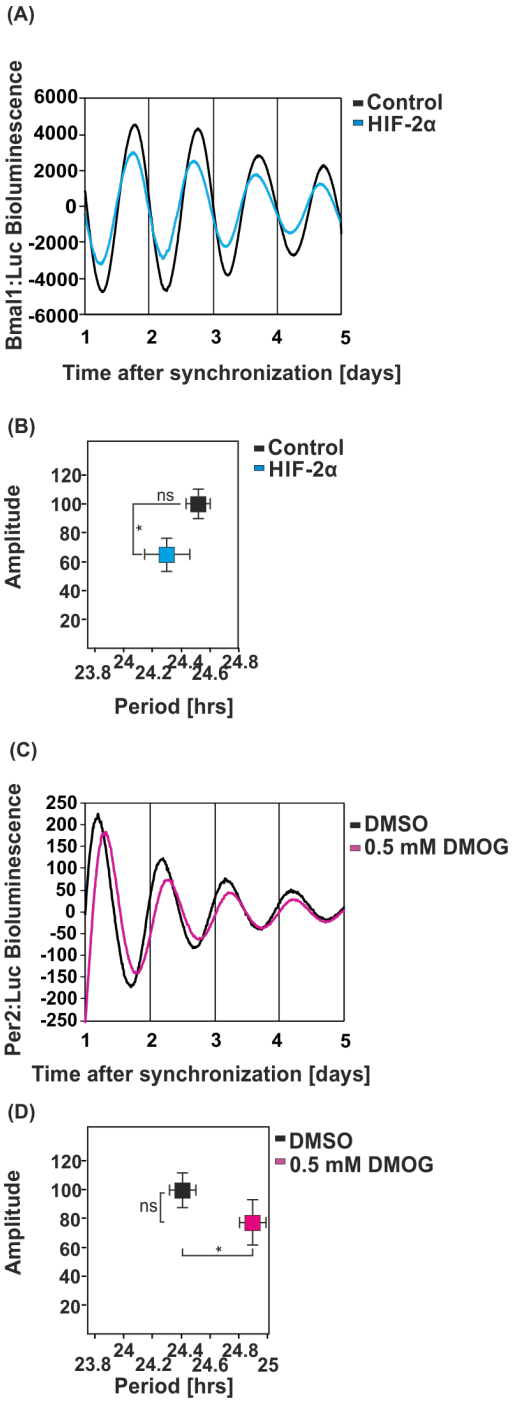

Figure S1 (refers to Fig.2)**. The circadian oscillation in NIH 3T3 cells is affected by HIF-2α and DMOG.** (A) Representative examples of the bioluminescence oscillations in NIH 3T3 cells cotransfected with an mBmal1:luciferase reporter construct and either empty vector (black line) or HIF-2α (blue line). (B) Graphical illustration of the amplitude (y-axis) and period length (x-axis) upon overexpression of HIF-2α. Data are mean ±SEM. * $p < 0.001$ (C) Representative examples of the bioluminescence oscillations in NIH $3T3^{mPer2:Luc}$ cells treated with DMSO as a mock and 0.5 mM DMOG. (D) Graphical illustration of the amplitude (y-axis) and period length (x-axis) upon DMOG treatment. Data are mean ±SEM. *$p < 0.05$.

Figure S1

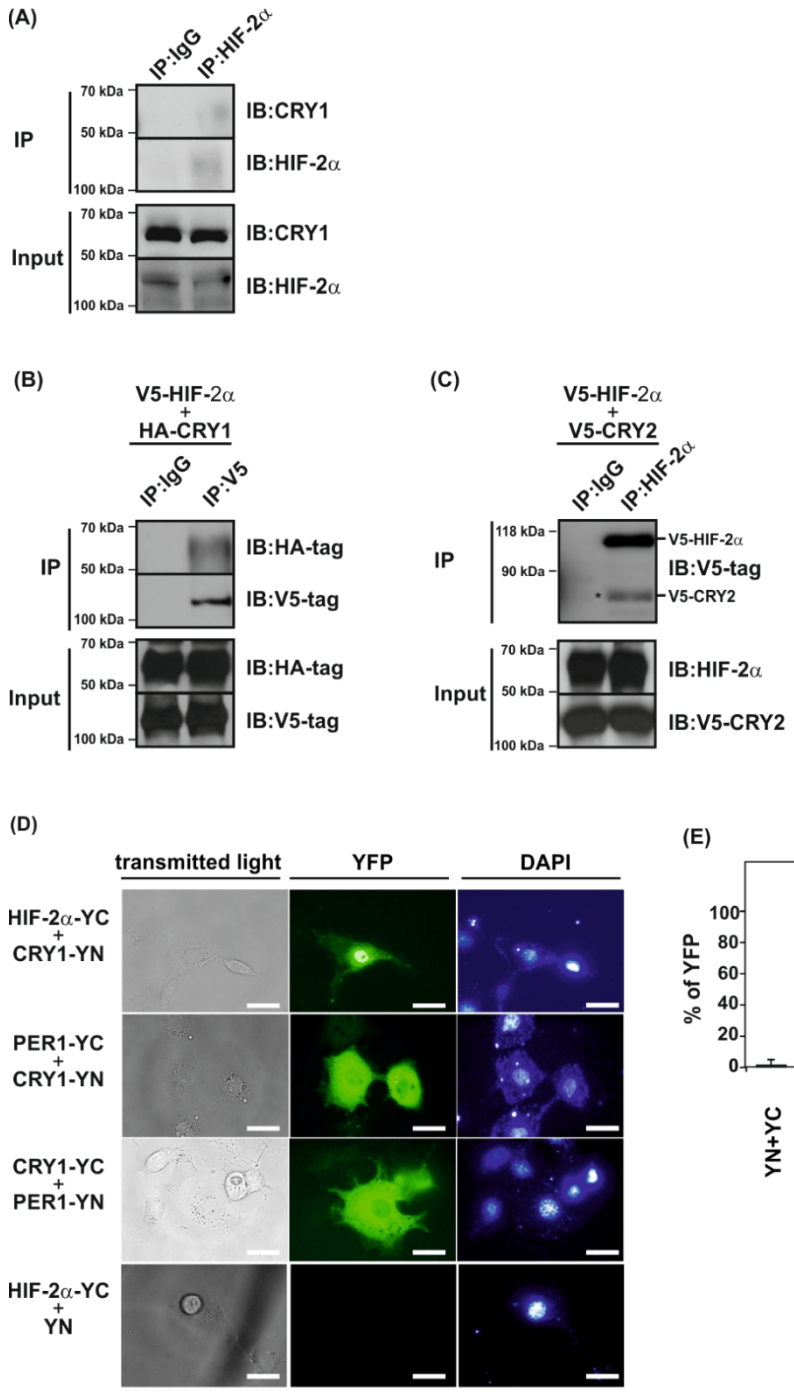

Figure S2

Figure S2 (refers to Fig.4)**. CRY1 interacts with HIF-2α.** (A) Coimmunoprecipitation assays (IPs) from wild-type (WT) MEFs cultured under hypoxia in the presence of MG-132. Blots from anti-HIF-2α IPs were probed with the CRY1 and HIF-2α antibody. The blots shown are representative of two independent experiments. (B, C) Co-immunoprecipitation assays with HEK-293 cells, expressing HIF-2α with either HA-tagged CRY1 or V5-tagged CRY2. (B) Blots from anti-V5 tag IPs were probed with HA-tag and V5-tag antibody. (C) Blots from anti-HIF-2α IPs were probed with V5-tag antibody (C*) Please note that both plasmids are V5-tagged. Therefore, the IPs were done with HIF-2α Abs and probed with anti V5-tag Abs thus resulting in recognition of both overexpressed proteins. (D) BiFC analysis. COS-7 cells cotransfected with the expression vectors for HIF-2α-YC, CRY1-YN, CRY-YC, PER-YN or PER-YC and a vector encoding only YN were cultured on glass slides for 24 hrs. The fluorescence detection was performed using specific filter sets for YFP and DAPI.
Scale bar: 10 µm. (E) Quantification of the BiFC signal. Cells were transfected as in (D) and quantified by flow cytometry (cf. Materials and Methods). The CMV-YFP signal was set to 100%. Data are mean ±SEM. * $p < 0.05$.

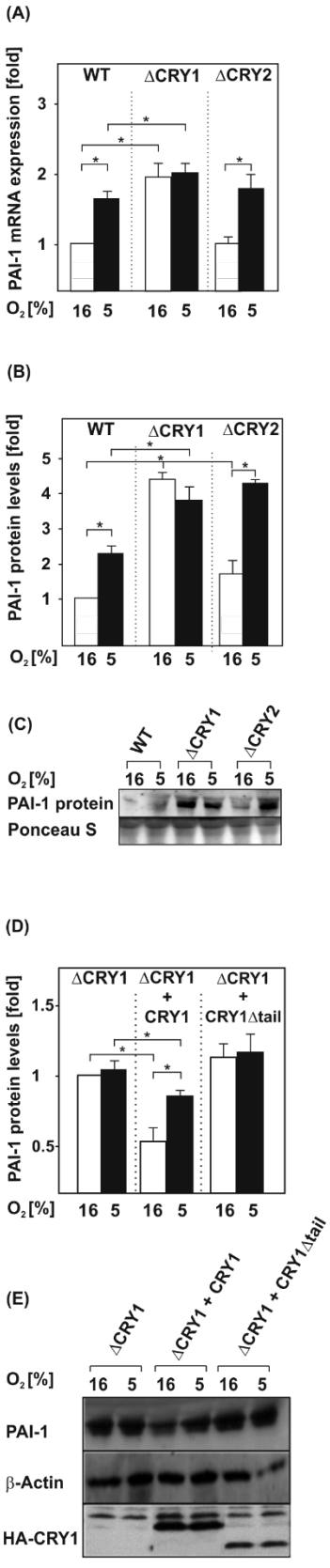

Figure S3 (refers to Fig.7A,B)**. CRY1 but not CRY2 modulates hypoxia-dependent transcription of PAI-1**. Wild-type (WT) MEFs, or MEFs deficient for CRY1 (ΔCRY1) or CRY2 (ΔCRY2) were cultured under normoxia (16% O_2) and hypoxia (5% O_2). The PAI-1 mRNA and protein levels were measured after 4 hrs and 24 hrs by qRT-PCR and Western blot, respectively. (A) Quantitative qRT-PCR data. (B) Quantification of the data from Western blots representatively presented in (C). The values under normoxia were set to 1. Values represent means ± SEM of at least three independent experiments. Statistics, Student's t-test for paired values: *significant difference, $p \leq 0.05$. (D, E) CRY1-deficient cells were transfected with a plasmid encoding CRY1 or CRY1-Δtail. The PAI-1 protein was measured by Western blot with an antibody against PAI-1. The values under normoxia were set to 1. Values represent means ± SEM of at least three independent experiments.

Statistics, Student's t-test for paired values: *significant difference, $p \leq 0.05$.

Figure S3

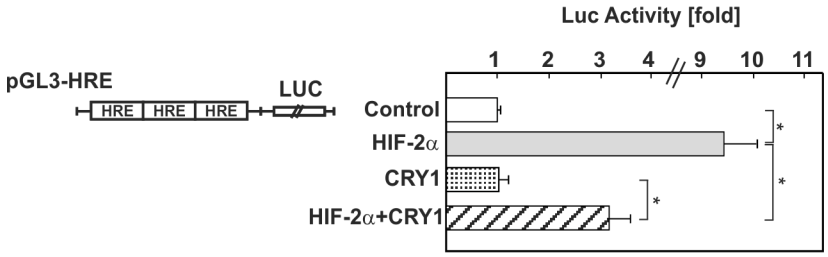

Figure S4

Figure S4 (refers to Fig.7C)**. HIF-2α-dependent transactivation of the HRE-driven promoter Luc construct is downregulated by CRY1.** Luciferase gene constructs containing 3 HIF-binding HREs (pGL3-HRE) in front of the SV40 promoter were cotransfected with expression vectors encoding CRY1, HIF-2α or both in combination. Cells were cultured under normoxia (16% O_2) and hypoxia (5% O_2) for 24 hrs before luciferase assay; In each experiment the Luc activity of pGL3-HRE transfected cells at 16% O_2 was set to 1. Values are means ± SD of four independent culture experiments, each performed in duplicate. Statistics, Student's t-test for paired values: *significant difference, $p \leq 0.01$.

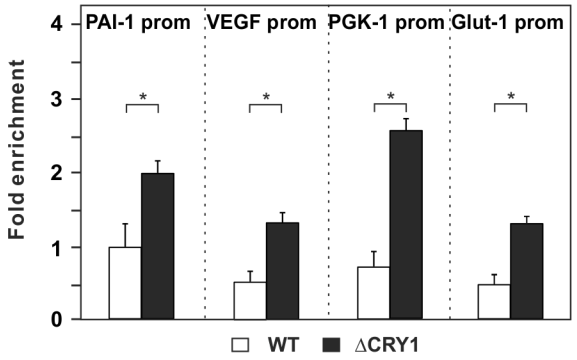

Figure S5

Figure S5 (refers to Fig.7D)**. Deficiency of CRY1 favors binding of HIF-2α to HRE-containing promoters.** ChIP-qPCR analyses were performed in wild-type or CRY1-deficient MEFs, cultured under hypoxia for 16 hrs; DNA fragments were co-precipitated with antibodies against mouse HIF-2α and amplified by qPCR using primers specific for the mouse PAI-1, VEGF-A, PGK-1 and GLUT-1 promoters. Chromatin immunoprecipitation without antibody or using IgG instead of antibody served as an additional specificity control. Differences in HIF-2α DNA binding efficiency in wild-type and ΔCRY1 MEFs were calculated by the fold enrichment method relative to the IgG control. Values are means ± SEM of three independent experiments. *significant difference, $p \leq 0.05$.

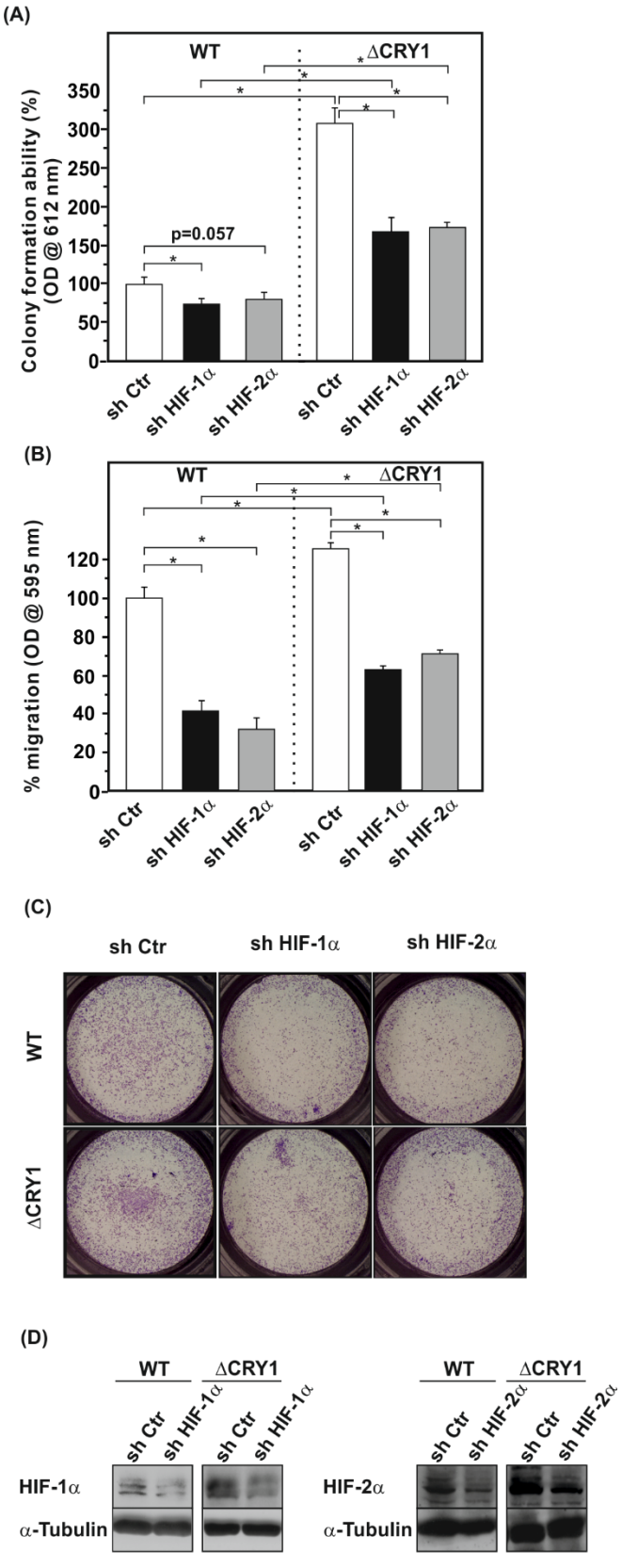

Figure S6 (refers to Fig.10)**. CRY1 and HIFs have opposite roles on cell proliferation and migration.** (A-D) Wild-type (WT) and CRY1-deficient (ΔCRY1) MEFs were transduced with retroviral particles expressing a scrambled non-coding shRNA (shCtr), a shRNA against HIF-1α or shRNA against HIF-2α. (A) Soft agar colony formation. Cells were plated onto soft agar and allowed to grow under hypoxia for 2 weeks. After staining with Resazurin the absorbtion was measured at an excitation wavelength of 584 nm and emission at 612 nm. The OD of the WT cells were set to 100%. Values represent means ± SEM of at least three independent experiments. (B) Transwell migration assay. Cells were seeded into Transwell chambers and incubated under hypoxia overnight. After staining with crystal violet the absorbtion of migrated cells at 595 nm was quantified. The OD of the WT cells was set to 100%. Values represent means ± SEM of at least two independent experiments. Statistics, Student's t-test for paired values: *significant difference, $p \leq 0.05$. (C) Representative photographs of a transwell migration assay. (D) Representative HIF-1α and HIF-2α Western blots in WT and ΔCRY1 MEFs transduced with respective HIF shRNA expressing retroviral particles.

Figure S6

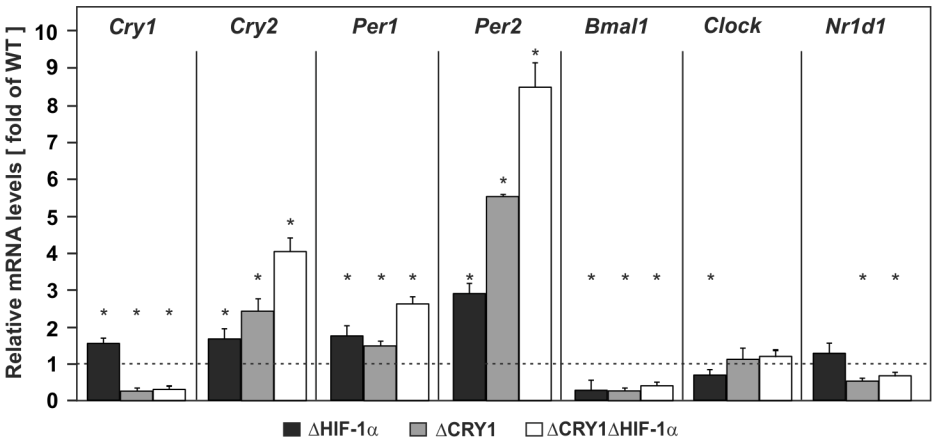

Figure S7

Figure S7 (refers to Fig.10)**. Lack of HIF-1α and CRY-1 regulates expression of clock genes.** Quantification of Cry1, Cry2, Per1, Per1, Bmal1, Clock, and Ndr1d1 mRNA levels in MEFs lacking either Cry1 (ΔCRY1), HIF-1α (ΔHIF-1α) or both (ΔCRY1ΔHIF-1α). The respective mRNA levels were assessed by qRT-PCR and the mRNA levels in wild type (WT) MEFs were set to 1; the values indicate fold-change WT vs the respective knockout. Data are mean ±SD (n=3), * significant difference WT vs. knockout.

Transparent Methods

All biochemical substances and enzymes used were of analytical grade obtained from commercial suppliers.

Animal experiments and monitoring of circadian behavior

All animal experiments were performed according to protocols approved by the National Animal Experiment Board of Finland following the regulations of the EU Directive 86/609/EEC, the European Convention ETS123 and the national legislation of Finland. Inbred C57BL/6N male mice were housed under standard conditions and fed *ad libitum*. For monitoring total physical activity (XT) of 2-month-old C57BL/6N mice under normoxia and hypoxia an automated infrared analyzing system for small animals (LabMaster, TSE Systems GmbH, Bad Homburg, Germany) was used. Before the real experiment the mice were housed individually for 7 days in training cages similar to those used in the actual measurements. Animals were maintained in a cycle of 12 hrs light and 12 hrs darkness (LD) or in continuous darkness (DD) in constant ambient temperature with water and food available *ad libitum*. The activity data were recorded continuously (every 10 min) for 2 weeks under normoxic or hypoxic conditions (17% O_2). All data are presented as a mean ± SEM, $p \leq 0.05$. Activity records were plotted as actograms (http://www.circadian.org/softwar.html) and the period of locomotor activity was determined by the cosinor and chisquare method. One-way Anova with post-hoc Tukey HSD Test, Mann Whitney test as well as Student's t-test were used to make statistical comparisons between the different conditions.

Cell Culture

HeLa, HepG2, COS-7 and HEK-293 cells were cultured in MEM (Sigma-Aldrich); mouse embryonic fibroblasts (MEFs) were cultured in DMEM (Sigma-Aldrich); NIH 3T3 and NIH 3T3 cell stably expressing a Per2:Luc construct (kindly provided by Hiroki R. Ueda [Isojima et al., 2009]) (were maintained in DMEM-Ham-F10 (1:1, Lonza); All cell culture media were supplemented with 10% fetal bovine serum (Biochrom), 1% nonessential amino acids (PAA Laboratories) and 0,5% antibiotics. The cells were cultured in a normoxic atmosphere of 16% O_2, 79% N_2, and 5% CO_2 [by volume] or a hypoxic atmosphere of 5% O_2, 90% N_2, 5% CO_2 [by volume], or in an InVivo2 400 hypoxia work station (Ruskinn Technologies).

Plasmids

For luminescence measurements the pGl4.11-Bmal1:luciferase (Bmal1:Luc) construct (kindly provided by Dr. U. Schibler, Geneva) (Brown et al., 2005), the reporter plasmids pGL3-hPAI-806/+19, containing the human PAI-1 promoter 5'-flanking region from -806 to +19 and the mutant pGL3-hPAI-806HREm (Dimova et al., 2005) as well as the pGL3-HRE and pGL3-HREm luciferase reporter plasmids containing 3 repeats of a wild-type HRE or mutant HRE, respectively, (Liu et al., 2004) were used as a reporters.

The expression plasmids encoding full-length HIF-1α with mutations in proline 402, proline 564, and asparagine 803 as well as full-length HIF-2α were already described (Flügel, Görlach & Kietzmann, 2012). The expression plasmids encoding HA-tagged wild-type CRY1 and HA-tagged CRY1 mutants HA-CRY1mutNLSc (with mutations in a bi-partite nuclear localization signal domain), HA-CRY1Dtail (deletion of the C-terminal tail), HA-CRY1ΔCC (deletion of the coiled-coil (CC) domain), HA-CRY1ΔCCmutNLSc (deletion of the CC domain and mutation in NLS), HA-CRY1ΔCCtail (deletion of the CC domain and tail), HA-CRY1ins 487 were already described (Chaves et al., 2006). The expression vectors for ARNT in p3XFLAG-Myc-CMV™-24 (Sigma-Aldrich) as well as the constructs for BiFC assays were cloned during the course of this study.

The wild-type human HIF-1α cDNA cloned into pCMV-Myc (Clontech) (Flugel et al., 2007) was used as a template to generate expression constructs for various HIF-1α mutants by using the OuickChange mutagenesis kit (Stratagene) followed by digestion and re-ligation (primer sequences are listed in Table S1). The HIF-1α variants are: bHLH (containing HIF-1α amino acids 1-80 encompassing the bHLH domain), bHLH-PAS A (containing HIF1α amino acids 1-200 and lacking PAS B, ODD, ID and CAD), bHLH-PASA-PASB (containing HIF-1α amino acids 1-350 and lacking ODD, ID and CAD), bHLH-PASA-PASB-ODD (containing HIF-1α amino acids 1-603 and lacking ID and CAD), bHLH-PASA-PASB-ODD-ID (HIF-1α amino acids 1-786 lacking the CAD), bHLH-ODD-ID-CAD (lacking PAS A and PAS B domains) and PAS A-PAS B-ODD-ID-CAD (lacking the bHLH domain). The constructs for production of retroviral particles expressing shRNA against Mus musculus HIF-1α (# TG517255), HIF-2α (# TF500609) and scrambled negative shRNA (# TR30013) were purchased from OriGene Technologies Inc. (Rockville, MD). The CRISPR-Cas9 backbone plasmid, pSpCas9(BB)-2A-GFP (PX458) (Addgene #48138) was a generous gift from Dr. Feng Zhang (Ran et al., 2013)

RNA preparation and quantitative real-time PCR

Isolation of total RNA was performed using the Qiagen RNeasy® Mini Kit (Qiagen, Switzerland) and with a GenElute mammalian total RNA miniprep kit (Sigma-Aldrich) following the manufacturer's instructions. Reverse transcription was conducted with 1 µg of total RNA and qScript cDNA Synthesis kit (Quanta Bioscience, GE Healthcare). Quantitative real-time PCR was performed in duplicate or triplicate using an iTaq Universal SYBR Green Supermix reaction kit (Biorad, Finland) and Applied Biosystems 7500 Real-Time PCR System (Life Technologies, Finland). All primer sets (Table S1) were validated for their product and amplification efficiency using standard dilution analysis and melting curve analysis. β-Actin, 18S rRNA and Hprt (hypoxanthine-guanine phosphoribosyltransferase) were used as internal controls to normalize the variability in expression levels. The relative quantification of gene expression was determined using the ΔΔCt method (Schmittgen, Livak, 2008, Livak, Schmittgen, 2001).

Transfections and real-time bioluminescence

HepG2 cells, 4 x 10^5 per 60-mm dish were transfected essentially as described (Immenschuh et al., 1998). In brief, 2 µg of the appropriate promoter Firefly luciferase (Luc) constructs were cotransfected in duplicate with 0,5 µg of the respective expression vector for HIFs, ARNT or CRY1, or with empty vector in the controls. After 5 hrs the medium was changed, and the cells were cultured under normoxia and/or hypoxia as indicated.

For real-time monitoring of the circadian oscillations in cell cultures, cell medium was buffered with 25 mM HEPES containing 0.1 mM luciferin (Sigma-Aldrich) for 2 days prior measurement. After synchronization of intracellular clocks by treatment of confluent cultures with 10 µM forskolin, plates were sealed and the bioluminescence was recorded for at least 5 days (75 sec measurements at 10 min intervals) with a LumiCycle 32-channel automated luminometer (Actimetrics). The data were analysed with the Actimetrics software using the running-average method and two sample comparisons were done using a paired Students t-test.

Western blot analysis, co-immunoprecipitations and HIF-1α protein half-life studies

Western blot analysis was carried out as described (Immenschuh et al., 1998). In brief, media or total cellular lysates were collected, and 100 µg of protein was loaded onto a 10% or 7.5% SDS-polyacrylamide gel and, after electrophoresis and blotting, probed with a primary monoclonal antibody directed against human HIF-1α (1:2000, Novus, Littleton, USA), myc-tag (1:1000, Cell Signaling, Frankfurt/M, Germany), or with a primary polyclonal antibody against HA-tag (1:500, Santa Cruz, Heidelberg, Germany), mouse HIF-1α (1:2000, Novus, Littleton, USA), CRY1 (H-84; 1:1000; Santa Cruz Biotechnology), Golgi membrane (1:10000; Biosciences, Goettingen, Germany), β-actin (1:10000, Sigma-Aldrich) and α-tubulin (1:10000, Sigma-Aldrich). The enhanced chemiluminescence system (ECL; Amersham Biosciences) was used for detection.

Co-immunoprecipitation experiments were performed either in hypoxic wild-type MEFs or in HEK-293 cells transiently transfected with full-length HA-tagged CRY1, V5-tagged CRY2, myc-tagged HIF-1α or V5-tagged HIF-2α. Twenty hours post-transfection total cellular protein extracts were isolated and 150 µg protein extracts were cleared with 2 µg of antibody pre-coupled to protein-G-Sepharose (Amersham, Freiburg, Germany). The samples were then subjected to Western blot analyses using anti-HIF-1α, anti-HIF-2α, anti-CRY1, anti-myc-tag, anti-V5tag or anti-HA-tag antibodies. HIF-1α half-life studies were performed under hypoxia in wild-type and ΔCRY1 MEFs treated with cycloheximide (10 µg/mL; Sigma-Aldrich). After harvesting the cells at the indicated time points, the endogenous HIF-1α protein levels were measured by Western blot.

BiFC analyses

For BiFC assays, pCMV-HA (Clontech) was used as a backbone for generation of the pCMV-YN, pCMV-YC, pCMV- HIF-1α-YC, pCMV-CRY1-YN and pCMV-ARNT-YN constructs; their correctness was proven by DNA sequencing. In brief, the sequences encoding HIF, ARNT and CRY were fused to sequences encoding YFP residues 1–154 (YN) or residues 155–238 (YC). The coding regions were connected by linker sequences encoding RSIAT (YN) or RPACKIPNDLKQKVMNH (YC) and were fused to the amino-terminal HA epitope tag in pHA-CMV (Clontech).

COS-7 cells were cultured in 6-well plates on glass slides to about 50% confluence and cotransfected with expression vectors pCMV-HIF-1α-YC and either pCMV-CRY1-YN, pCMV-ARNT-YN or pCMV-YN (2,5 µg each). The fluorescence was observed 24 h post-transfection using an inverted fluorescence microscope (Carl Zeiss AxioVert 200M). YFP fluorescence was captured using an excitation wavelength of 500 nm and an emission

wavelength of 535 nm. The nuclei of fluorescent cells were stained with 4′,6-diamidino-2-phenylindole dihydrochloride (DAPI).
Quantification of the BiFC Signal was perfomed by flow cytometry. In brief, cells were transfected as above and 48 hrs post transfection cells were washed with PBS and harvested by trypsin-EDTA. Cells were then pelleted by centrifugation at 1000 rpm for 2 min. The cell pellet was resuspended in 1.5 ml of PBS. The BiFC signal was quantified using the CyFlow Space flow cytometer equipped with an appropriate filter set for YFP. In each case, triplicates of 5000 cells were counted and used to calculate the average BiFC signal intensity in each sample using the FloMAX software. The fluorescence for maximal fluorescence in each experiment, against which The BiFC signal intensities were normalized against the signal from full-length YFP which was set to 100%.

Chromatin immunoprecipitation
ChIP analyses were carried out according to the protocol for fast ChIP (Nelson, Denisenko & Bomsztyk, 2006). In brief, confluent wild-type and DCRY1 MEFs cultured under normoxia or hypoxia for 16 hrs were crosslinked with formaldehyde, lysed, and sonicated to obtain DNA fragments in a size from 250 to 500 bp. Then, chromatin was precipitated with a mouse HIF-1α, HIF-2α antibody (Novus, Littleton, USA) or unspecific IgG. DNA from chromatin immunopreciptiations was analyzed by quantitative real-time PCR. Differences in the HIF-1α and HIF-2α DNA binding efficiency in wild-type and ΔCRY1 MEFs were calculated by the fold enrichment method relative to the IgG control using the formula $2^{-(Ct\ [IP] - Ct\ [IgG])}$.

Generation of HIF-1α knockout MEFs by CRISPR-Cas9-mediated genome editing
A 20-bp guide sequence targeting the third exon of mouse HIF-1α (HIF-1α-001, ENSMUST00000021530.7) was designed online using Zhang's laboratory web resource (www.genome-engineering.org); a non-targeting, scrambled sequence (OriGene) was used as a negative control. gRNA-encoding oligonucleotides (Sigma-Aldrich) were cloned into the vector SpCas9(BB)-2A-GFP (PX458, Addgene plasmid ID 48138) using standard procedures as described (Ran et al., 2013). The generation of the HIF-1α control and knockout cells via CRISPR-Cas9-mediated non-homologous end-joining (NHEJ) DNA repair and the screening was performed according to described guidelines (Ran et al., 2013). In brief, the wild-type and ΔCry1 MEFs were transiently transfected with either the genome editing or the scrambled CRISPR-Cas9 construct and 48 hrs post-transfection cells were subjected to single-cell-sorting (BD FACSAria™ III cell sorter). The single-cell clones were expanded and screened for frame-shift mutations; shortly, a region spanning the target site was amplified by PCR from genomic DNA isolated from clonal cell lines. PCR products were subsequently cloned into pUC19 (Invitrogen). 15-20 sequences were analyzed per clone by aligning them to the WT HIF-1α sequences using BLAST and Serial Cloner. All primer sequences are listed in Table S2.

Live Cell Imaging Assays
For real-time quantitative live-cell proliferation analysis, $5x10^3$ cells per well were seeded onto 96-well plates. Live phase contrast recording of cell confluence was performed in the IncuCyte® ZOOM System (Essen BioScience) for 72 h in 3 h intervals. For the scratch wound assays, $4x10^4$ cells per well were seeded onto 96-well Essen ImageLock Plates (Essen Bioscience) in the presence of a proliferation inhibitor (mitomycin, 1µg/ml). The following day the confluent cell monolayer was wounded with the 96 PTFE pin Wound Maker (Essen Bioscience) and the live wound closure was recorded for 45 h in 3 h intervals. In both assays, the confluence analyses were performed using the basic IncuCyte software settings.

Colony formation
Anchorage-independent growth was analyzed in a three-layer soft agar assay as described (Flügel, Görlach & Kietzmann, 2012). In brief, the $1x10^3$ cells per well were seeded in triplicates and incubated at 37°C for 14 days under normoxia and/or hypoxia before the colonies were visualized with resazurin or crystal violet. Cell growth was measured in a Fluroskan Ascent FL type 374 (Thermo Scientific) with an excitation wavelength of 584 nm and emission at 612 nm.

Transwell migration assay
Cell migration assays were conducted *in vitro* in transwell chambers (Becton Dickinson) as described (Flügel, Görlach & Kietzmann, 2012). In brief, serum-starved cells were seeded into the top chamber at a density of $2x10^4$ cells/well in 500 µl of serum-free DMEM; the bottom chamber was filled with 600 µl DMEM containing 10% FBS.

After 18 hrs in a humidified hypoxic incubator, cells were fixed and stained with crystal violet. The absorption of migrated cells at 595 nm was quantified.

Satistics

Statistical analyses were performed with GraphPad Prism version 5 (GraphPad Software). Parameters and experimental details can be found in the figure legends. The Student's t test with a p-value of at least $p \leq 0.05$ was considered statistically significant.

Table S1. (refers to Fig.6) **Primers used for generation of HIF-1α deletion constructs.** The wild-type human HIF-1α cDNA cloned into pCMV-Myc vector (Clontech) was used as a template for generating expression constructs for different HIF-1α mutants. The OuickChange mutagenesis kit (Stratagene) was used to introduce restriction enzyme sites and/or stop codon (underlined) and was followed by digestion and re-ligation. The antisense primers contained the reverse complementary sequence of the sense primer. The correctness of all designed deletion mutants was proven by DNA sequencing.

Construct	(bp)	Sequence (5'- 3') of the sense mutagenesis primers	Deleted domain	digest
bHLH	**243**	ctggatgctggtgattagggtaccgaagatgacatgaaagcacag	PAS A, PAS B, ODD, ID, CAD	*Kpn I*
bHLH-PAS A	**528**	gcgaagctttttctctgaatgtagggtaccctaactagccg	PAS B, ODD, ID, CAD	*Kpn I*
bHLH-PAS APAS B	**1215**	cctgatgctttaacttagctggtaccagccgctggagacac	ODD, ID, CAD	*Kpn I*
bHLH-PAS A-PAS B- ODD	**1830**	cagtattccagtagactcaggtaccagaacctactgctaatgccacc	ID, CAD	*Kpn I*
bHLH-PAS A-PAS B- ODD-ID	**2379**	ctgctggggcaatcataggatgaaagtggggtaccacagctgacc	CAD	*Kpn I*
bHLH-ODD-IDCAD	**1800**	gctatttgcgtgtgaggaagcttctggatgctggtg ggacaagtcaccacaggaaagcttaggatgcttgccaaaagagg	PAS A, PAS B,	*Hind III*
PAS A-PAS B-ODD-ID-CAD	**2238**	ggtgatttggatattgaagaggccatggaggcccagatgaa	bHLH	*Sfi I*

Table 2S. (refers to Fig.4, 7, 10) **Primer sequences**

Gene/ Construct	Forward (5'-3')	Reverse (5'-3')
qPCR primers		
Pai-1	GTGAATGCCCTCTACTTCAGTG	GCTGCCATCAGACTTGTGGAA
Hif1α	GGGGAGGACGATGAACATCAA	GGGTGGTTTCTTGTACCCACA
Hif2α	TCCTTCGGACACATAAGCTCC	GACAGAAAGATCATGTCACCGT
ActB	GTTGTCGACGACGAGCG	GCACAGAGCCTCGCCTT
18S rRNA	GTAACCCGTTGAACCCCATT	CCATCCAATCGGTAGTAGCG
Hprt	CGAAGTGTTGGATACAGGCC	GGCAACATCAACAGGACTCC

Cited2	CGCCAGGTTTAACAACTCCCA	TGCTGGTTTGTCCCGTTCAT
Glut1	CTCTGTCGGCCTCTTTGTTAAT	CCAGTTTGGAGAAGCCCATAAG
Cry1	CACTGGTTCCGAAAGGGACTC	CTGAAGCAAAAATCGCCACCT
Cry2	CACTGGTTCCGCAAAGGACTA	CCACGGGTCGAGGATGTAGA
Per1	TGAAGCAAGACCGGGAGAG	CACACACGCCGTCACATCA
Per2	GAAAGCTGTCACCACCATAGAA	AACTCGCACTTCCTTTTCAGG
Bmal1	TGACCCTCATGGAAGGTTAGAA	GGACATTGCATTGCATGTTGG
Clock	CTTCCTGGTAACGCGAGAAAG	GTCGAATCTCACTAGCATCTGAC
Nr1d1	ATGTCCCGAGAGCTACATGAC	CCTGCTCCTGAACATCGAACT
BiFC		
pCMV-YC	CGAATTCAAGCTTCTCGAGACGCGTATGGGTAC	CCATACGCGTCTCGAGAAGCTTGAATTCGGGCC
pCMV-YN	AATTCGGGCCCACGCGTGGTACCT	TAGAGGTACCACGCGTGGGCCCG
pCMV-CRY1YC	GAATTCAAGCATGGGGGTGAACGCCGTGC	GGCCCTCTAGAGTTACTGCTCTGCC
pCMV-HIF-1α -YC	CTGAAGCTTGCGGCCGCACGTCCGGCGTGCAAAATC	CATGCAAGCTTCGCGGGTACAATTCCGCAGCTTTTAG
ChIP primers		
Pai-1	GTCTAGACGACCGACCAGCCAAA	GAAATGTCTGGGCTGCCCGC
Pgk-1	GGCATTCTGCACGCTTCAA	GAAGAGGAGAACAGCGCGG
Glut-1	ATTTCTAAGGCCCTGGGTCC	CCTGCCTGATGCGTGTCA
Vegf-A	CAGTTGTCTCTCCTTCAGGGCT	GAAACCCACGTATGCACTGTGTA
ActB	GTGAGTGAGCGACGCGGAGCCAA	CTTACCTGGTGGCGGGTGTGGA
CRISPR-Cas9		
Hif1 (guide)	GCTAACAGATGACGGCGACA	
Hif1a (genotyping, sequencing)	CACCCTTGGTGATTTGCTTGT	CCTCATGGTCACATGGATGAGT
Hif1a	GATATGAATTCACCCTTGGTGATTTGCTTGT	CGATAAGCTTCCTCATGGTCACATGGATGAGT
(pUC19 cloning, sequencing)		
Rom1 (off-target)	GGTGGGAAGGGGAAAGATGG	ACAGTGATTTCTGTCCACAAACTT

References

Brown SA, Ripperger J, Kadener S, Fleury-Olela F, Vilbois F, Rosbash M, Schibler U. 2005 “PERIOD1-associated proteins modulate the negative limb of the mammalian circadian oscillator”. *Science.* vol. 29; no. 308(5722), pp. 693-6.

Chaves, I., Yagita, K., Barnhoorn, S., Okamura, H., Van Der Horst, G.T.J. & Tamanini, F. 2006, "Functional evolution of the photolyase/cryptochrome protein family: Importance of the C terminus of mammalian CRY1 for circadian core oscillator performance", *Molecular and cellular biology,* vol. 26, no. 5, pp. 1743-1753.

Dimova, E.Y., Moller, U., Herzig, S., Fink, T., Zachar, V., Ebbesen, P. & Kietzmann, T. 2005, "Transcriptional regulation of plasminogen activator inhibitor-1 expression by insulin-like growth factor-1 via MAP kinases and hypoxia-inducible factor-1 in HepG2 cells", *Thrombosis and haemostasis,* vol. 93, no. 6, pp. 1176-1184.

Flügel, D., Görlach, A. & Kietzmann, T. 2012, "GSK-3beta regulates cell growth, migration, and angiogenesis via Fbw7 and USP28-dependent degradation of HIF-1alpha", *Blood,* vol. 119, no. 5, pp. 1292-1301.

Flügel, D., Görlach, A., Michiels, C. & Kietzmann, T. 2007, "Glycogen synthase kinase 3 phosphorylates hypoxiainducible factor 1alpha and mediates its destabilization in a VHL-independent manner", *Molecular and cellular biology,* vol. 27, no. 9, pp. 3253-3265.

Immenschuh, S., Hinke, V., Ohlmann, A., Gifhorn-Katz, S., Katz, N., Jungermann, K. & Kietzmann, T. 1998, "Transcriptional activation of the haem oxygenase-1 gene by cGMP via a cAMP response element/activator protein-1 element in primary cultures of rat hepatocytes", *The Biochemical journal,* vol. 334 (Pt 1), no. Pt 1, pp. 141-146.

Isojima Y, Nakajima M, Ukai H, Fujishima H, Yamada RG, Masumoto KH, Kiuchi R, Ishida M, Ukai-Tadenuma M, Minami Y, Kito R, Nakao K, Kishimoto W, Yoo SH, Shimomura K, Takao T, Takano A, Kojima T, Nagai K, Sakaki Y, Takahashi JS, Ueda HR. 2009 “CKIepsilon/delta-dependent phosphorylation is a temperatureinsensitive, period-determining process in the mammalian circadian clock.” *Proceedings of the National Academy of Sciences of the United States of America,* vol. 106 no 37, pp. 15744-15749.

Liu, Q., Berchner-Pfannschmidt, U., Moller, U., Brecht, M., Wotzlaw, C., Acker, H., Jungermann, K. & Kietzmann, T. 2004, "A Fenton reaction at the endoplasmic reticulum is involved in the redox control of hypoxia-inducible gene expression", *Proceedings of the National Academy of Sciences of the United States of America,* vol. 101, no. 12, pp. 4302-4307.

Livak, K.J. & Schmittgen, T.D. 2001, "Analysis of relative gene expression data using real-time quantitative PCR and the 2(-Delta Delta C(T)) Method", *Methods (San Diego, Calif.),* vol. 25, no. 4, pp. 402-408.

Nelson, J.D., Denisenko, O. & Bomsztyk, K. 2006, "Protocol for the fast chromatin immunoprecipitation (ChIP) method", *Nature protocols,* vol. 1, no. 1, pp. 179-185.

Ran, F.A., Hsu, P.D., Wright, J., Agarwala, V., Scott, D.A. & Zhang, F. 2013, "Genome engineering using the CRISPR-Cas9 system", *Nature protocols,* vol. 8, no. 11, pp. 2281-2308.

Schmittgen, T.D. & Livak, K.J. 2008, "Analyzing real-time PCR data by the comparative C(T) method", *Nature protocols,* vol. 3, no. 6, pp. 1101-1108.